THEORETICAL AND EXPERIMENTAL STUDY OF THE PHOTOVOLTAIC EFFECT IN THIN FILMS

A Thesis

Presented to the

School of Graduate Studies

Addis Ababa University

In Partial Fulfilment

of the Requirements for the Degree

of Master of Science in

Physics

by

Gebre Hiwet Embaye

June, 1985

ADDIS ABABA UNIVERSITY

School of Graduate Studies

THEORETICAL AND EXPERIMENTAL STUDY OF THE PHOTOVOLTAIC EFFECT IN THIN FILMS

by

Gebre Hiwet Embaye
Faculty of Science

Approved by the Examining Board:

Dr. Andreas Brauer External Examiner	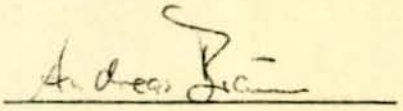
Dr. P. Hrushka Advisor	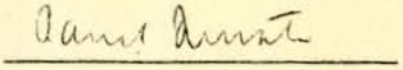
Dr. A. Spartakov Member	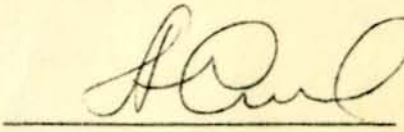
Dr. V. Schepilov Chairman	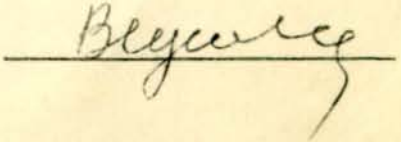

ACKNOWLEDGEMENTS

I would like to express my heartfelt thank to my Instructor and Advisor, Dr. P. Hruska, for his effort in guiding and supervising this work.

I am also thankful to Ato Eskinder Seyoum who spent his precious time and energy for typing the first draft of this whole manuscript. My thanks are also due to my firend Ato Mihret Getu of Flora Project who restlessly went through the manuscript for typographic errors. His technical assistance is also unforgetable.

DEDICATION

This work is totaly dedicated to my beloved wife,

Tsadkan Zebello

TABLE OF CONTENTS

LIST OF TABLES

LIST OF FIGURES

ABSTRACT

In the present study the theory of photovoltaic energy conversion is presented. Basic factors affecting conversion capability of photovoltaic devices are discussed. General formula of the minority carrier distribution and current density across p-n junctions are revised and further developed to arrive at the over all collection efficiency expression which is valid for any thin film photovoltaic cells. Focuss is put on the main solar cell parameters like conversion efficiency and spectral response.

To the end some experimental works on a single crystal solar cell (FD-K) are made. Emphasis is put on establishing circuits capable of measuring various solar cell parameters ranging from Si-single crystal cell of low efficiency. The results of the measurement are presented in the form of tables and graphs. Conclusions are also made on the results obtained.

Up to the present time tremendous efforts have been made by many scholars involved in the field to improve solar-photovoltaic conversion efficiencies. Single crystal solar cells for which efficiency measurements in the range of 5% to 18%, and thin film polycrystalline solar cells of efficiencies between 5% to 9% were reported upto the year 1978 [9].

The efficiencies reported considerably depend on the methods used during the processing of the devices and also on the types of the materials used. For example, high efficiency electroplated heterojunction thin film solar cell (Cds/CdTe) was reported by Bulent M. Basol in 1984 [10] while in the same year Cds/CdTe thin film solar cell fabricated by the close-spaced-sublimation (CCS) process had higher efficiency (>10%) [11].

The over-all efficiency comparisons between single crystal solar cells and thin film polycrystalline solar cells places the former in the superior position. However, there is no fundamental barrier to the achievement of higher efficiencies in thin film cells and, indeed, their limiting efficiency should in principle be comparable to the efficiencies achieved and achievable in single crystal cells.

From the economic point of view the production of single crystal cells of the required purity involves an inherently expensive process while thin film solar cells could be produced

at a relatively lower cost technology. Thus, the real future of photovoltaic energy conversion appears to be closely connected with the possibility of producing thin film photovoltaic cells.

The general objective of the present thesis work focuses on studying the main characterstics of thin film photovoltaic generators and the factors which affect their performance. To this end, the paper is organized in such a way that the first chapter entails the general theory of photovoltaic effect in thin film solar cells. In the second chapter, the various factors which affect photovoltaic solar energy conversion performance are discussed. Analytical treatment of the transport problem of excess minority carriers in single crystal p-n junction is revised and utilized for further developing the over-all collection efficiency (spectral response) expression in this chapter. The next two chapters summarize the main functions and characterstics of electrical connections and environmental interfaces of a generalized thin film solar cells and the design options in the present time solar cell production. The final chapter embodies the experimental measurements carried on a given sample solar cell (Si) which was in our disposal. Its efficiency, spectral response, current-voltage, and capacitance-voltage measurements are given, and calculations of the barrier-height, and donor density in the dark and under illumination are made.

The fabrication of a thin layer solar cell by electroplating method according to B.M. Basol [10] which was originally planned, could not be realized, because of lack of certain chemicals. An attempt to produce a photoelectrochemical cell according to Ki Hyun Yoon [12] was not also successful because Titanium sheet was not available. The obstacles mentioned above led us to perform a thorough theoretical and experimental study of the solar cell.

CHAPTER 1

THE THEORY OF PHOTOVOLTAIC EFFECT (PVE) IN THIN FILMS

PVE is the generation of an electromotive force (EMF) by the absorption of light (or ionizing radiation) in an inhomogeneous solid. It is distinguished from localized heating which can cause an EMF via thermoelectric effects or the Dember effect which results from non-uniform illumination in a homogeneous solid.

1.1. Necessary conditions for PVE occurrence.

In order for a PVE to occur in a system, the following criteria must be fulfilled.

Light must be absorbed in the semiconductor and mobile excess carriers must be generated as a result of the absorption; the light generated excess carriers must be separated by a built-in electrostatic field (built-in potential barrier); and the lifetime of the excess carriers must be long enough to allow them to travel from the places where they are generated to the charge separation site.

1.1.1. Light absorption.

Absorption takes place when photons are incident on the solar cell provided that their energy is greater than the band gap.

The ability of a material to absorb light of a given wavelength is measured quantitatively by the absorption coefficient α, measured in units of reciprocal distance. Light at the surface of solar cells falls off in intensity, by a factor of 1/e for each $1/\alpha$ distance into the material. As a general rule, the wider the band gap, the smaller the value of α for a given wavelength. The absorption coefficient also depends on the densities of states in the conduction and valence bands |13| and the directness and indirectness of the band gaps.

1.1.2. Charge Separation.

As soon as absorption takes place electrons are raised in energy from the valence band to the conduction band, creating electron-hole pairs. These light generated carriers must then be separated by a built-in electrostatic field so that they can diffuse to the edges of the space-charge region before they recombine. As a result of this field they are swept across the junction giving rise to a photocurrent, photovoltage and power to a desired load.

This barrier is merely a result of electronic inhomogeneity in the system; and is usually called the electronic junction. It is the site of the potential barrier which is necessary for a photovoltaic device.

The junction can be 1) a p-n junction (homojunction) made of one type of semiconductor material with two opposite types

of conductivity; 2) a heterojunction composed of two different semiconductors; 3) a Schottky barrier which is a metal semiconductor (MS) junction or 4) a metal-insulator-semiconductor (MIS) junction.

1.1.3. Carrier lifetime.

The excess carriers generated as a result of the absorption of ionizing radiation must remain free long enough to travel from the point of generation to the charge separation site.

Once an electron has been optically excited to the conduction band leaving a hole in the valence band, it may either recombine with a hole or migrate to the edge of the semiconductor and be collected for useful work. The collection of photogenerated carriers across the p-n junction is in competition with the loss of these carriers by bulk and surface recombination before they can be collected. Bulk recombination can occur by direct mutual anhilation of a free electron and a free hole or by anhilation through an intermediate recombination center.

The intermediate recombination is usually the dominant mechanism. If there are N_r recombination centers located at an energy level E_r and having capture cross-sections σ_n, σ_p for an electron when empty and for a hole when filled, then

the hole-life time on the n-side of the junction can be described by [13].

$$\tau_p = \frac{1}{\sigma_p V_{th} N_r}\left[\left(1 + \frac{N_c}{n_{no}} e^{-\left(\frac{E_c - E_r}{KT}\right)}\right) + \left(\frac{\sigma_p}{\sigma_n}\right)\left(\frac{N_v}{n_{no}}\right) e^{-\left(\frac{E_r - E_v}{KT}\right)}\right]$$

where N_c, N_v are the number of conduction and valence electrons; n_{no} is the free electron concentration on the n-type side and is essentially equal to the doping level, v_{th} is the thermal velocity, K is the Boltzman constant, and E_c and E_v are the conduction and valence band edges, respectively. An analogous equation can be obtained for the electron life-time in p-type material. The actual life times are determined by a multiplicity of such recombination centres at a number of energy levels, but qualitatively, this equation indicates that the life time will decrease with increasing doping level and saturates at a value equal to

$$\tau_{po} = (\sigma_p V_{th} N_r)^{-1} \qquad (1.2)$$

In addition to a recombination in the bulk, a loss of photogenerated minority carriers also takes place at the surface of the material due to the presence of surface states which arise from dangling bonds, chemical residues, metal precipitates, native oxides, and the like [13].

The rate at which carriers are lost at a surface is described by the surface recombination velocity S which is related with the minority-carrier current density towards the surface by

$$J_{surface} = q\, S_p\, (p_n - p_{no}) \tag{1.3}$$

for holes in an n-type material and

$$J_{surface} = q\, S_n (n_p - n_{po}) \tag{1.4}$$

for electrons in a p-type material. $p_n - p_{no}$, $n_p - n_{po}$ are the excess carriers in the n and p type material respectively.

If the surface diffusion length $L_{S_{p,n}}$ for holes and electron is known the hole and electron life-times and the corresponding surface recombination velocities $S_{p,n}$ could be related as

$$\tau_{p,n} = \frac{L_{S_{p,n}}}{S_{p,n}} \tag{1.5}$$

For specimens that have a high concentration of impurities, the scattering is frequent, the mean free paths are short, and the mobilities are low. Crystals that are heavily doped usually have low mobilities in the extrinsic temperature range. Imperfections in the crystal arise due to dopants, vacancies, dislocations in the bulk. These together with imperfections on the surface act as recombination centers and thus decrease the diffusion length and life-times of the electron-hole carriers.

As decisive as these imperfections are to the cause of recombination effects in single crystals, their effects are highly pronounced in thin films. Because, thin films usually contain far more bulk defects in single crystals made from the same semiconductor, and because recombination at the grain boundaries can severely limit solar cell performance.

1.2. The effects of grain boundaries on the carrier life time in polycrystalline thin films

A thorough analysis of grain boundary effects on both the photocurrent and dark current in thin film solar cells has never been carried out as far as our knowledge of the problem is concerned. A complete analysis of this problem entails a three dimensional solution to the diffusion equation with eight boundary conditions. Partial solution for the simpler case of uniform generation of minority carriers throughout a volume of rectangular filament has been achieved by [14] where he used his analysis to define a "filament life-time" made up partly of the bulk life time in the filament and partly of surface recombination life time in the filament. When the filament dimensions are small and the surface recombination velocities are high, the recombination in the filament is dominated by the surface terms and the "filament life time" is much smaller than the bulk life time. Similar considerations apply to polycrystalline film, which can be thought as many filaments connected in parallel and sometimes in series.

Fig.1.1. Energy profile in the vicinity of grain boundaries.

If Figure 1.1, an energy profile at and around grain boundaries is shown. Theoretically, it appears that grain boundaries act as minority carrier sinks (surface of high recombination velocity) and majority carrier barriers, thus reduce the photocurrent, increase the dark current, decrease the shunt resistance and increase the series resistance.

One possible combination of grain boundaries is where a random orientation of the grains prevail as shown in Fig.1.2.

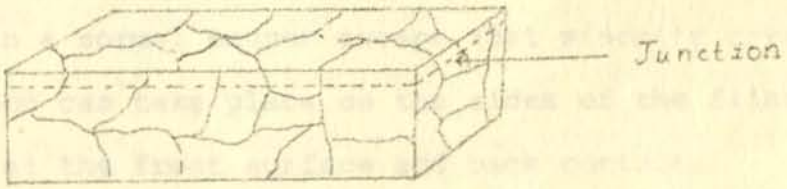

Fig.1.2. Random orientation of grains.

In such a situation only the top most grain or two grains will be able to contribute to the output; the grains which are below are effectively isolated from the junction by the grain

boundaries above them. This gives the series combination of grain boundaries in which the effective carrier life time in the film will be very low and the device will behave very poorly.

Another possible orientation of the grains is a fibrous epitaxial type as shown in figure 1.3.

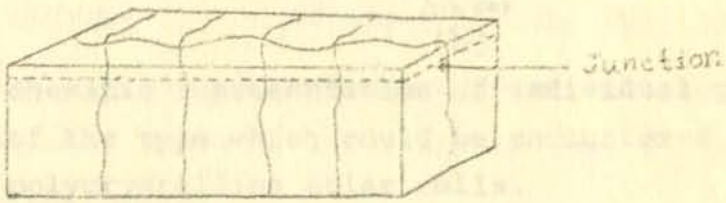

Fig.1.3. Fibrous epitaxial orientation of grains

In such thin film structures, minority carriers within each filament can cross the junction boundary and the whole layer thickness can contribute to the output. In such a situation the over all solar cell can be thought of as a parallel combination of filamentary solar cells, each of which act in a normal manner except that minority carrier recombination can take place on the sides of the filaments as well as at the front surface and back contact.

A schematic representation of individual grains in polycrystalline thin film solar cells is shown in figure 1.4 where the surfaces of the grain are characterized by surface recombination velocities: S_s for the surface on which the light is incident; S_{gb} for the surface of the grain boundary. At an ohmic contact S is infinite.

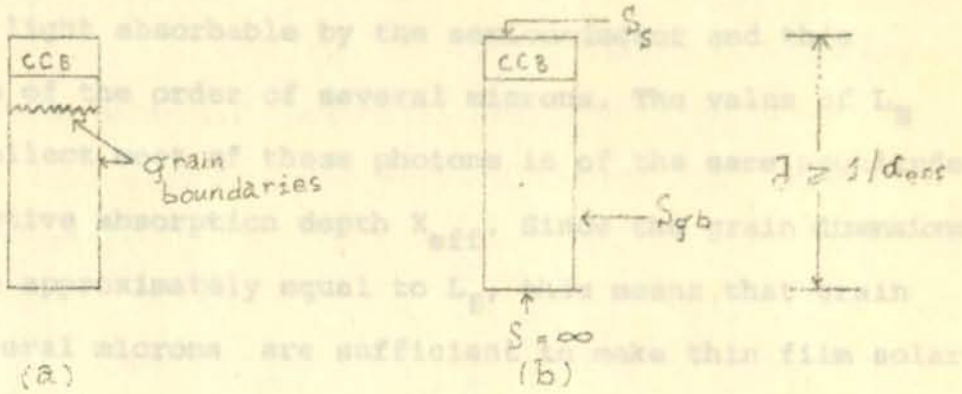

Fig.1.4. Shematic representation of individual grains of the type which could be encountered in polycrystalline solar cells.

The presence of a grain boundary parallel to the major surface area of a grain as shown in figure 1.4a reduces the grain dimensions and thus carriers generated by photons absorbed in the region below this grain boundary can not migrate to the charge collection barrier (CCB).

As regards the vertical grain boundaries and how they affect recombination, shockley treated the transport problem of minority carries injected into a filament of rectangular cross-sections |14|. He showed that the effective diffusion length of minority carriers traversing the filament was equal to the bulk diffusion length of the filament provided that the filament dimensions were equal to or greater than the bulk diffusion length L_B, even if the recombination velocity at the grain boundaries, S_{gb}, is infinity. This conclusion has important consquences with respect to the selection of semiconductors for thin film cells. Substantially

thinner films of direct gap semiconductors are needed to absorb most of the light absorbable by the semiconductor and this thickness is of the order of several microns. The value of L_B needed to collect most of these photons is of the same magnitude as the effective absorption depth X_{eff}. Since the grain dimensions need only be approximately equal to L_B, this means that grain sizes of several microns are sufficient to make thin film solar cells from direct gap semiconductor whose recombination properties should be comparable to those of large single crystal cells made from the same semiconductors.

In the case of an indirect gap semiconductors like Si, Ge, etc. however, the effective absorption depth is of the order of a hundred microns and required grain dimensions are of this same order.

This simple examination of the problems associated with grain boundaries and their recombination effect illustrates the advantage of direct gap semiconductors for use in thin film cells.

Surface recombination losses could be minimized by increasing the grain dimensions. Other approaches involved application of appropriate chemicals which alter the defect structure at the surface.

A phenomenally successful approach is the one suggested by J.J. Loferski [9]. It involves the incorporation of minority carrier mirrors (MCM) i.e. potential barriers which drive minority carriers away from the surface towards the charge collection barrier.

CHAPTER 2

THE FACTORS AFFECTING PHOTOVOLTAIC SOLAR ENERGY CONVERSION PERFORMANCE

In this chapter the main factors which limit the photovoltaic energy converter performance will be elaborated, and possibilities for their improvement will be discussed. Throughout the discussion the five-layered generalized thin film solar cell will be borne in mind.

The generalized thin-film solar cell can be thought to consist of 1) an encapsulant antireflecting coating, 2) a transparent ohmic contact, 3) an absorber-generator semiconductor layer, 4) a collector-converter semiconductor layer, and 5) an opaque ohmic contact as schematically shown in Figure 2.1.

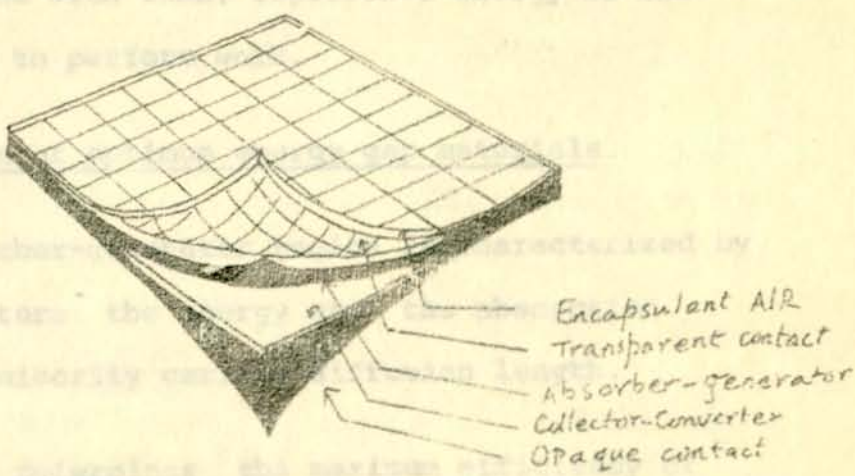

Fig.2.1. A five layered generalized thin film solar Cell.

2.1. Semiconductor Layers

The essential features of any solar cell are an

absorber-generator material in which mobile carriers are generated by the absorption of light, and a built-in potential region which allows the generated carriers to be collected from the region in which they were generated and converted to majority carriers. This collector-converter prevents the back flow of carriers.

The absorber-generator region determines the magnitude of the current that is generated and the height of the potential battier determines the voltage the cell can produce. In some structures the absorber-generator can be in the region where the transition to the voltage differential occurs, the space-charge region.

The product of voltage and current creates the power which, when integrated with time, represents energy of the source which is able to perform work.

2.1.1. Selection of optimum energy gap materials.

The photon absorber-generator region is characterized by the following parameters: the energy gap, the absorption coefficient and the minority carrier diffusion length.

The energy gap determines the maximum efficiency of the cell that can be achieved utilizing a single absorber-generator. Incident photons in the solar spectrum with an energy equal to or greater than the energy gap excite free carriers (electron-hole pairs) and determine the maximum obtainable

current that can be generated. The maximum voltage is also determined by the energy gap of the absorber-generator and the characterstics of the junction formed with the collector-converter.

Figure 2.2 below shows the dependence of conversion efficiency on the energy gap as given by |9|. It gives a guidance as to the wide choice of materials for an absorber-generator. On the same figure, an approximate dependence of the short-circuit current and the open-circuit voltage on the energy gap is shown.

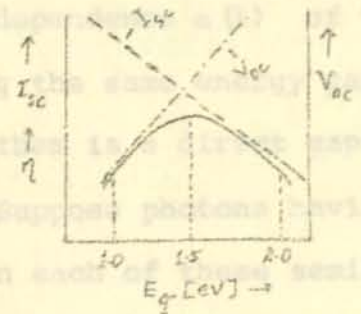

$\eta \propto I_{sc} V_{oc} \times$ Fill Factor

$I = \int_{E_g}^{\infty} n_{ph}(h\nu)\, Q(h\nu, \alpha, S, d, L)\, d(h\nu)$

$V_{oc} = \frac{AkT}{q} \ln\left(\frac{I_{sc}}{I_o} + 1\right)$

$I_o \propto k \exp\left(-\frac{E_G}{BkT}\right)$; $B \sim A$

Fig.2.2. The approximate dependence of I_{sc}, V_{oc} and η on energy gap of the semiconductor comprising the solar cell.

2.1.2 Selection of Optimum Thickness

It is necessary to define the limits of thickness that qualify a semiconducting material as a thin film solar cell, for the absorption capability of materials, among many other possible factors, depends upon the thickness of the absorber-generator layer.

Consider a beam of light having wavelength λ , normally incident on a semiconductor having an absorption constant $\alpha(\lambda)$ for this particular wavelength. Then the flux of photons $N_{ph}(X)$ remaining in the beam after it traverses a thickness X of semiconductor is given by

$$N_{ph}(X) = N_{ph}(0)\ e^{-\alpha(\lambda)} \qquad (2.1)$$

where $N_{ph}(0)$ is the normally incident photon flux.

The wavelength dependence $\alpha(\lambda)$ of two hypothetical semiconductors having the same energy gap E_G are shown in figure 2.3. One of them is a direct gap, the other an indirect gap semiconductor. Suppose photons having energy $E_G + \Delta E$ be incident normally on each of these semiconductors. If the respective thickness of each of them is X_d and X_i, then according to equation (2.1)

$$\frac{X_i}{X_d} = \frac{\alpha^{(d)}}{\alpha^{(i)}} \qquad (2.2)$$

where $\alpha^{(d)}$ and $\alpha^{(i)}$ are the absorption constants for photons of energy $E_G + \Delta E$ in the direct and indirect gap materials respectively.

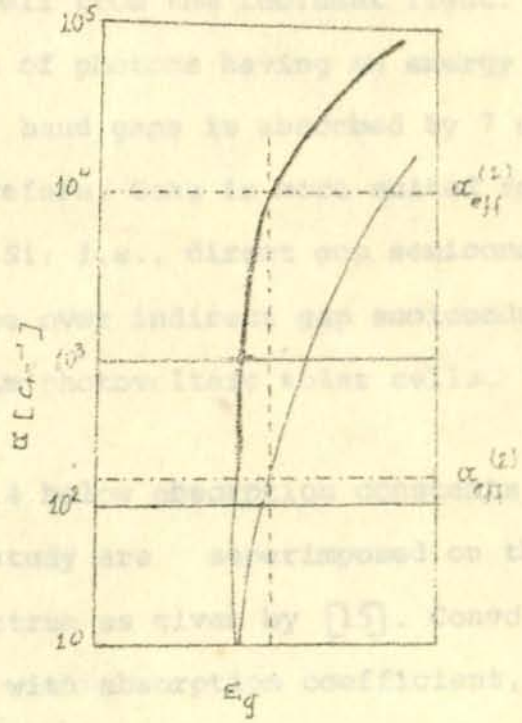

Fig.2.3. Hypothetical absorption characterstics (α versus $h\nu$) for two semiconductors (1-direct, 2-indirect) having the same energy gap.

For illustration purposes, consider the direct gap semiconductor GaAs ($E_G \simeq 1.35$ eV) and the indirect gap semiconductor S_i ($E_G \simeq 1.1$ eV). For $E = 0.2\ E_G$, X_{eff} is about 7 μm (14 μm optical path length) for GaAs and about 500 μm (1000 μm optical path length) for si. The power output of a photovoltaic cell is proportional to the power absorbed in the cell from the incident light. Approximately the same fraction of photons having an energy in excess of their respective band gaps is absorbed by 7 μm of GaAs and 50 μm of Si. Therefore, GaAs is more suited for thin film solar cells than Si; i.e., direct gap semiconductors have distinct advantage over indirect gap semiconductors as the basis of thin film photovoltaic solar cells.

In figure 2.4 below absorption constants for the materials presently under study are superimposed on the photon flux of the solar spectrum as given by [15]. Convoluting the spectral density with absorption coefficient, one finds that the only material with energy gap between 1.0 and 1.7 eV which cannot absorb 90% of the photons, say, in a 5 μm thick film is crystalline silicon. Crystalline silicon will absorb 70% of the photons in a 10 μm thickness and 90% of the photons in a 100 μm thickness.

In contrast to silicon, many of the materials will absorb 90% of the available sunlight in thickness less than 1 μm, e.g., Copper Sulphide will absorb 90% of this sunlight above its energy gap with a thickness of only 0.4 μm.

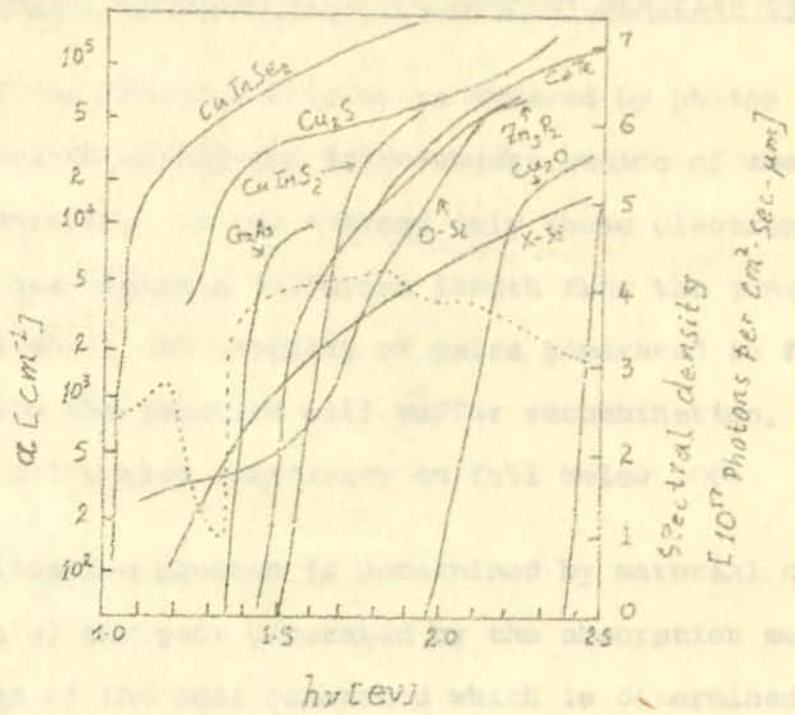

Fig.2.4. Thin film solar cell materials absorption coefficient versus photon energy.

Therefore, materials with the ability to absorb light in thinner layers are best candidates for thin film photovoltaic energy converters, for they given the prime answer to economic concerns.

2.2. The transport problem of the generated minority carriers.

Most of the electron-hole pairs created by photon absorption are not generated within the space-charge region of the p-n junction. Therefore, on the average only those electron-hole pairs which are within a diffusion length from the junction will be collected while the majority of pairs generated in far away distances from the junction will suffer recombination, thus causing the collection efficiency to fall below 100%.

The collection process is determined by material constants: the location of the pair generated by the absorption mechanism, the diffusion of the pair generated which is determined by mobility, and recombination which is determined by minority carrier life time.

In this section a general analytical evaluation of the collection process which was carried by |16| will be revised in detail, and will be developed to obtain the spectral response expressions.

The assumptions made are a uniform n-p or p-n junction; constant mobility, life time and doping.

2.2.1. Evaluation of minority carrier distribution

A one dimensional model is considered throughout. The number of photons absorbed per unit time in a unit area of a layer of

thickness dx at a distance x below the surface is given by Lambert's law of absorption as

$$g(x)dx = \alpha N e^{-\alpha x} dx \qquad (2.3)$$

where this gives the number of electron-hole pairs generated.

The continuity equation for excess holes above the equilibrium density in an n-type material is given by

$$\frac{\partial p}{\partial t} = \frac{-p}{\tau} + D_p \frac{\partial^2 p}{\partial x^2} + \alpha N e^{-\alpha x} \qquad (2.4)$$

where $\frac{\partial p}{\partial t}$ is the rate of change of minority carriers (holes) in the n-type material, $\frac{-p}{\tau}$ is the recombination rate of minority carriers in excess of the equillibrium density P_n, $D_p \frac{\partial^2 p}{\partial x^2}$ is the diffusion rate into (out of) the layer under consideration.

For solar energy conversion, the steady state case is of interest. Thus, one obtains from (2.4)

$$D_p \frac{d^2 p}{dx^2} - \frac{p}{\tau} + \alpha N e^{-\alpha x} = 0 \qquad (2.5)$$

Using Einstein's relation between diffusion length L, diffusion constant D, and minority carrier life time τ i.e.

$$L = (D\tau)^{\frac{1}{2}} \qquad (2.6)$$

in equation (2.5), the following expression is obtained.

$$\frac{d^2 p}{dx^2} - \frac{1}{L_p^2} p + \frac{\alpha N}{D_p} e^{-\alpha x} = 0 \qquad (2.7)$$

Solution of this inhomogeneous differential equation is evaluated as follows. First we find the solution for the homogenous part:

$$\frac{d^2p}{dx^2} - \frac{1}{L_p^2} p = 0 \qquad (2.8)$$

which has a complementary solution p_c given by

$$p_c = p_1 e^{\frac{x}{Lp}} + p_2 e^{\frac{-x}{Lp}} \qquad (2.9)$$

The particular solution p_p which will satisfy equation (2.7) is

$$p_p = Ae^{\alpha x} \qquad (2.10)$$

where A is determined by substituting equation (2.10) and its spatial second-derivative into equation (2.7) and p_p is found to be

$$p_p = - \frac{N}{\alpha D_p (1 - \frac{1}{\alpha^2 L_p^2})} e^{-\alpha x} \qquad (2.11)$$

Thus, the general solution to the differential equation given in (2.7) is

$$p = p_c + p_p \qquad (2.12)$$

i.e.

$$p = p_1 e^{\frac{1}{L_p}x} + p_2 e^{-\frac{1}{L_p}x} - \frac{NNe^{-\alpha x}}{\alpha D_p (1-1/\alpha^2 L_p^2)} \qquad (2.13)$$

For the minority carriers (electrons) in p-type material, equivalent expression exists

$$n = n_1 e^{\frac{1}{L_n}x} + n_2 e^{-\frac{1}{L_n}x} - \frac{N e^{-\alpha x}}{\alpha D_n (1-1/\alpha^2 L_n^2)} \qquad (2.14)$$

The constants p_1, p_2, n_1, n_2 are determined from the following set of boundary conditions:

1) At $x = 0$, surface recombination takes place which is given by

$$D_n \left(\frac{dn}{dx}\right)_{x=0} = S_n n(0) \qquad (2.15)$$

2) At $x = x_j$ is a p-n junction kept in the zero-bias condition leading to short-circuit current so that a perfect sink for minority carriers exist. This is expressed as

$$n(x_j) = p(x_j) = 0 \qquad (2.16)$$

3) Surface recombination also takes place at the back surface that is at $x = d$. This is expressed as

$$D_p \left(\frac{dp}{dx}\right)_{x=d} = S_p p(d) \qquad (2.17)$$

Frequently ohmic contacts are applied to this surface so that in such cases S_p tends to infinity.

Using the boundary conditions (1) and (2) as follows,

$$D_n \left(\frac{dn}{dx}\right)_{x=0} = S_n n(0) \tag{2.15}$$

yields

$$\left(\frac{D_n}{L_n} - S_n\right) n_1 + \left(\frac{D_n}{L_n} + S_n\right) n_2 = -N \left(\frac{1}{1 - \frac{1}{\alpha^2 L_n^2}} + \frac{1}{\alpha D_n (1 - 1/\alpha^2 L_n^2}\right) \tag{2.18}$$

and

$$n(x_j) = 0 \tag{2.16}$$

yields

$$\left(e^{\frac{1}{L_n} x_j}\right) n_1 + \left(e^{\frac{1}{L_n} x_j}\right) n_2 = \frac{N e^{-x_j}}{\alpha D_n (1 - 1/\alpha^2 L_n^2} \tag{2.19}$$

Solving (2.18) and (2.19) simultaneously for n_1 and n_2 we obtain the following expressions

$$n_1 = \frac{-e^{\frac{1}{L_n} x_j} N \left[1 - \frac{1}{1/\alpha^2 L_n^2} + \alpha D_n \left(1 - \frac{1}{1/\alpha^2 L_n^2}\right)\right] - \left(\frac{D_n}{L_n} - S_n\right) \alpha D_n \left(1 - \frac{1}{1/\alpha^2 L_n^2}\right) \frac{N e^{-\alpha x_j}}{\alpha D_n}}{e^{-\frac{1}{L_n} x_j} \left(\frac{D_n}{L_n} - S_n\right) + \left(\frac{D_n}{L_n} + S_n\right) e^{\frac{1}{L_n} x_j}} \tag{2.20}$$

$$n_2 = \frac{e^{\frac{1}{L_n}x_j}\left[1 - \frac{1}{1/\alpha^2 L_n^2} + \frac{1}{D_n(1-1/\alpha^2 L_n^2)}\right] + \left(\frac{D_n}{L_n} - S_n\right)\alpha D_n\left(1 - \frac{\frac{N e^{-x_j}}{1}}{1/\alpha^2 L_n^2}\right)}{\left(\frac{D_n}{L_n} + S_n\right)e^{\frac{1}{L_n}x_j} + \left(\frac{D_n}{L_n} - S_n\right)e^{-\frac{1}{L_n}x_j}} \qquad (2.21)$$

with the following notations employed,

$$x'_n = \frac{x_n}{L_n}\ ;\quad y_n = \frac{x_j}{L_n}\ ;\quad a_n = \frac{S_n L_n}{D_n}\ ;\quad b_n = \alpha L_n$$

$n = n(x'_n, \lambda)$ becomes as follows where λ-dependence comes through α and N.

$$n(x'_n, \lambda) = \alpha(\lambda)\tau_n N(\lambda)\left\{\frac{1}{b_n^2-1}\left[e^{-x'_n}e^{(1-b_n)y_n} - e^{(1-b_n)x'_n}\right]\right.$$

$$\left.+\left[\frac{a_n+1}{b_n^2-1}\left(e^{(1-b_n)y_n} - 1\right) - \frac{1}{b_n+1}\right]\cdot\frac{\sinh(x'_n-y_n)}{\cosh y_n + a_n \sinh y_n}\right\}$$

for $b_n \neq 1$. (2.22)

In a similar manner, applying boundary conditions (2) and (3), one obtains

$$p(x'_p,\lambda) = \alpha(\lambda)\tau_p N(\lambda)\left\{\frac{1}{b_p^2-1}e^{-x'_p}\left[e^{(-b_p)y_p} - e^{(1-b_p)x'_p}\right]\right.$$

$$\left.+\left[\frac{a_p+1}{b_p^2-1}\left(e^{(1-b_p)(z-y_p)} - 1\right) - \frac{1}{b_p+1}\right]\cdot\frac{\sinh(x'_p-y_p)e^{-b_p z}}{\cosh(z-y_p) - a_p\sinh(z-y_p)}\right\}$$

for $b_p \neq 1$. (2.23)

The notations used here are

$$x'_p = \frac{x}{L_p};\quad y_p = \frac{x_j}{L_p};\quad z = \frac{d}{L_p};\quad a_p = \frac{S_p L_p}{D_p};\quad b_p = \alpha L_p$$

τ_n and τ_p are the life times and D_n , D_p the diffusion coefficients for minority carriers in the p- and n- layer respectively. $L_n = (D_n\tau_n)^{\frac{1}{2}}$, $L_p = (D_p\tau_p)^{\frac{1}{2}}$ are the diffusion lengths and S_n, S_p are the surface recombination velocities on the p- and n-type surfaces. x is the distance from the light exposed p-type surface and x_j is the distance from the surface to the p-n junction which is assumed to be infinitesimally thin.

Since equations (2.22) and (2.23) are indeterminate for the case $b(= \alpha L) = 1$, their forms for this case are obtained by taking the limit as $b \to 1$ and found to be as follows.

$$n(x'_n\ ,\ \lambda)b_n \to 1 = \tfrac{1}{2}\alpha(\lambda)\tau_n N(\lambda)\ \{-(y_n - x'_n)\ e^{-x'_n}$$

$$+\left[(a_n+1)y_n+1\right]\ \frac{\sinh(y_n - x'_n)}{\cosh\ y_n + a_n \sinh\ y_n}\} \qquad (2.24)$$

and

$$p(x'_p\ ,\ \lambda)b_p \to 1 = \tfrac{1}{2}\alpha'(\lambda)\tau_p N(\lambda)\ \{(x'_p - y_p)\ e^{-x'_p}$$

$$-\left[(a_p+1)(z-y_p)+1\right]\ \frac{\sinh\ (x'_p - y_p)\ .\ e^{-z}}{\cosh(z-y_p) - a_p \sinh(z-y_p)}\}$$

(2.25)

Equations (2.22), (2.23), (2.24) and (2.25) can be evaluated after the material constants and dimensions are determined, which can be readily done on prepared solar cells for all of these quantities except τ_n and τ_p.

2.2.2. Evaluation of the photocurrent density

The gradient of the minority carrier distributions near the junction due to photon absorption gives rise to a current flow across the junction. The magnitude of this currents can be evaluated from equations 2.23 and 2.24 as follows.

The electron current density, $j_n(\lambda)$, from the p-layer is obtained by

$$j_n(\lambda) = qD_n \left(\frac{dn}{dx}\right)_{x=x_j} \tag{2.26}$$

which yields

$$j_n(\lambda)\ qN(\lambda)b_n \left\{\frac{1}{b_n+1} e^{-b_n y_n} + \frac{1}{b_n^2-1} \cdot \frac{e^{(1-b_n)y_n} - b_n + a_n(e^{(1-b_n)y_n} - 1)}{\cosh y_n + a_n \sinh y_n}\right\}$$

$$\text{for } b_n \neq 1 \tag{2.27}$$

and

$$j_n(\lambda)b_n \to 1 = \tfrac{1}{2}qN(\lambda)\left\{e^{-y_n} - \frac{1+(1+a_n)y_n}{\cosh y_n + a_n \sinh y_n}\right\} \qquad (2.28)$$

The corresponding hole current density, $j_p(\lambda)$, from the n-layer is obtained by

$$j_p(\lambda) = -qD_p\left(\frac{dp}{dx}\right)_{x=x_j} \qquad (2.29)$$

which yields

$$j_p(\lambda) = -qN(\lambda)b_p\left\{\frac{1}{b_p+1}e^{-b_p y_p} + \frac{e^{-b_p z}}{b_p^2-1} \cdot \frac{e^{-(1-b_p)(z-y_p)} - b_p + a_p\left(e^{-(1-b_p)(z-y_p)} - 1\right)}{\cosh(z-y_p) - a_p \sinh(z-y_p)}\right\} \qquad (2.30)$$

for $b_p \neq 1$

and

$$j_p(\lambda)b_p \to 1 = -\tfrac{1}{2}qN(\lambda)\left\{e^{-y_p} - e^{-z}\,\frac{1-(1+a_p)(z-y_p)}{\cosh(z-y_p) - a_p \sinh(z-y_p)}\right\} \qquad (2.31)$$

Equations (2.30) and (2.31) reduce, for the case of ohmic contact covering the back surface of the wafer ($S_p \to \infty$) to the following expressions.

$$j_p(\lambda)a_p \to \infty = -qN(\lambda)b_p \left\{\frac{1}{b_p+1} e^{-b_p y_p} - \frac{e^{-b_p z}}{b_p^2-1} \cdot \frac{e^{-(1-b_p)(z-y_p)}-1}{\sinh (z-y_p)}\right. \quad (2.32)$$

$$\text{for } b_p \neq 1$$

and

$$j_p(\lambda)a_p \to \infty = -\tfrac{1}{2}N(\lambda) \left\{e^{-y_p} - e^{-z} \frac{z-y_p}{\sinh(z-y_p)}\right\} \quad (2.33)$$

$$\text{for } b_p = 1$$

The total light generated current density j_L is then given as

$$j_L = \int_o^\infty \left[j_n(\lambda) + j_p(\lambda) \right] d\lambda \quad (2.34)$$

2.2.3. Collection efficiency (spectral response)

The collection efficiency which is defined as the ratio of electron-hole pairs separated by the electric field of the p-n junction to the total number of electron-hole pairs generated and designated as η_{coll} is given as

$$\eta_{coll}(\lambda) = \frac{j_n(\lambda) + j_p(\lambda)}{qN(\lambda)(1-e^{-\alpha(\lambda)d})} \quad (2.35)$$

where the term in parenthesis in the denominator takes account of the fraction of photon transmitted through the wafer.

This collection efficiency takes into account only the incomplete collection of the electron-hole pairs by diffusion to the p-n junction.

The over-all collection efficiency $\Gamma(\lambda)$ which takes care of the reflection losses on the surface, the incomplete absorption of photons ($h\omega < E_g$) and the incomplete collection of the electron-hole pairs by diffusion to the p-n junction could be defined as

$$\Gamma(\lambda) = \frac{j_n(\lambda) + j_p(\lambda)}{qN_{inc}} \tag{2.36}$$

The relationship between the photon flux in the light beam, $N_{inc}(\lambda)$, and that actually entering the semiconductor, $N(\lambda)$, is determined by the reflection coefficient $r(\lambda)$ as follows

$$N(\lambda) = N_{inc}(1-r(\lambda)) \tag{2.37}$$

Inserting (2.37) into (2.35) we obtain

$$\eta_{coll} = \frac{j_n(\lambda) + j_p(\lambda)}{qN_{inc}(1-r(\lambda))(1-e^{-\alpha(\lambda)d})} \tag{2.38}$$

combining (2.36) and (2.38)

$$\Gamma(\lambda) = \frac{j_n(\lambda) + j_p(\lambda)}{qN_{inc}} = (1-r(\lambda)(1-e^{-\alpha(\lambda)d})\eta_{coll} \tag{2.39}$$

Improvement in collection efficiency for any given material could be achieved by increasing the minority carrier life time in the p- and n-materials, by using materials with higher electron and hole mobilities or by using materials with some what smaller absorption coefficients in the peak region of the solar spectrum.

2.3. Losses due to the I-V characterstics

2.3.1. The voltage factor (V.F.)

The amount of energy utilized in the generation of electron-hole pairs is equal to the potential difference between the top of the valence band and the conduction band. The largest recoverable voltage is however the open-circuit voltage which is lesser than the energy gap, mainly due to the following two reasons.

Firstly, the barrier height is determined by the difference in Fermi levels in the n- and p-type material on both sides of the junction. These Fermi levels are dependent on temperature and impurity concentration, and are normally located within the forbidden gap in the case of non-degenerate semiconductors. Thus, the barrier height (V_b) is less than the energy gap (E_g).

Another reason is the fact that a voltage equal to V_b will only be obtained at extremely high injection levels which are not reached by photon absorption from direct sunlight.

From the I-V characterstics of a p-n junction the maximum open-circuit voltage (V_{oc}) is given as

$$V.F. = V_{oc} = \frac{AKT}{q} \ln \left(\frac{I_L}{I_o} + 1\right) \qquad (2.40)$$

where I_o is saturation current, I_L is the light generated current or the short-circuit current (I_{sc}) and A is the so called perfection constant of the I-V characterstic.

The voltage factor (V.F.) is then defined as

$$V.F. = \frac{V_{oc}}{E_g} = \frac{AKT}{qE_g} \quad \ell n \quad (\frac{I_L}{I_o} + 1) \qquad (2.41)$$

From diffusion theory of p-n junctions as given by |17|

$$A = 1$$

and

$$I_o = qe^{-39E_g} \cdot (\sqrt{\mu_p/\tau_p} \cdot 1/N_d + \sqrt{\mu_n/\tau_n} \cdot 1/N_a) \qquad (2.42)$$

where A and I_o are exclusively determined by material constants and temperature. N_d, N_a are the donor and acceptor densities; μ_n, μ_p are electron and hole mobilities; and τ_n, τ_p are electron and hole life times.

2.3.2. The curve factor (C.F.)

The maximum power can be extracted from a photovoltaic device at that point for which the largest rectangle can be inscribed into the I-V characterstics (curves). This point is given by

$$P_{max} = V_{max} I_{max} \qquad (2.43)$$

and the curve factor is given by

$$C.F. = \frac{V_m I_m}{V_{oc} I_{sc}}$$

$$= \left[1 - \frac{AKT}{qV_{oc}} \ln\left(1+\frac{qV_m}{AKT}\right)\right] \cdot \left[1 - \frac{I_o}{I_{sc}} \exp\left(\frac{qV_m}{AKT} - 1\right)\right] \qquad (2.44)$$

where V_{oc} is given by equation (2.40), and

$$V_m = \left(1 + \frac{qV_m}{AKT}\right) \exp\left(\frac{qV_m}{AKT}\right)$$

$$= \frac{V_{sc}}{I_o} + 1$$

$$= \exp\left(\frac{qV_{oc}}{AKT}\right) \qquad (2.45)$$

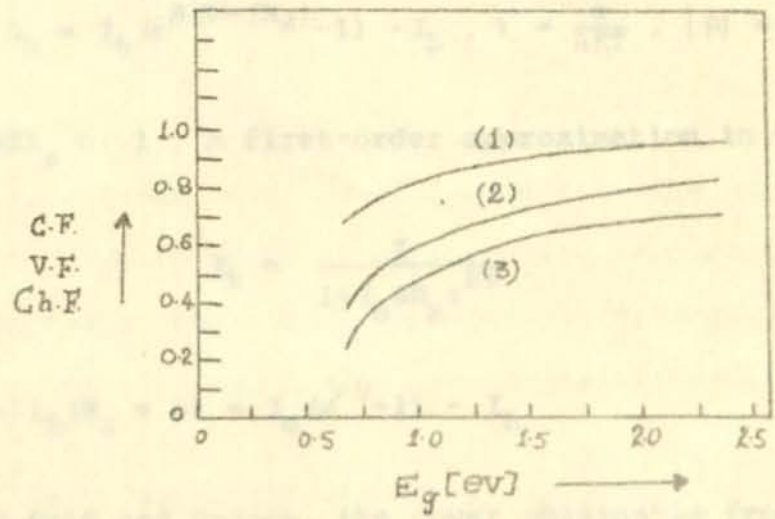

Fig.2.5. V.F., C.F., and Ch.F. versus width of energy gap. Published data by Wolf |16|.

The curve factor as well as the voltage factor are determined by the saturation current I_o. Better values of V.F. and C.F. are obtained at larger energy gaps as can be seen from figure 2.5.

The characterstic factor (CH.F.) which is defined as the product of V.F. and C.F. is given by

$$\text{CH.F.} = \text{V.F} \times \text{C.F} = \frac{V_m I_m}{E_g I_{sc}} \qquad (2.46)$$

The characterstic factor could be improved by proper choice of materials with suitable energy gap and selection of proper doping levels.

2.3.3. Series resistance losses

The output current from a solar cell is given by

$$I_R = I_o (e^{B(V-IR_s)} - 1) - I_L \;,\; B = \frac{q}{AKT} \;,\; |B| = V^{-1} \qquad (2.47)$$

If $BIR_s < 1$, a first-order approximation in the expo-term yields

$$I_R = \frac{I}{1 + I_o B R_s e^{BV}} \qquad (2.48)$$

where $I = I_R (R_s = 0) = I_o (e^{BV} - 1) - I_L$

Following Wolf and Prince, the power obtainable from a solar cell is

$$P = I_R V = I_R \frac{1}{B} \ln \left(\frac{I_L + I_R}{I_o} + 1 \right) + I_R^2 R_s \qquad (2.49)$$

where $I_R^2 R_s$ is the power dessipated directly in the series resistance R_s. The first term also bears dissipation due to variation of the I-V curve. Hence it could be imagined a total power dissipation P_{R_s} to exist.

2.4. Conversion efficiency (η) and limit conversion efficiency ($\eta_{\ell im}$)

Combining all the loss factors so far discussed we reach at the so called conversion efficiency, which is the one obtainable in practice.

$$\eta = \frac{P_{out}}{P_{in}} = (V.F.)\,(C.F.)\,(1-P_{R_s})\,\frac{q}{hc}\int_0^\infty [1-r(\lambda)]$$

$$\cdot\,[1-e^{-\alpha(\lambda)d}]\,\eta_{coll}(\lambda)\,P_{in}(\lambda)\;d\lambda$$

$$\cdot\left[\int_0^\infty P_{in}(\lambda)\,d\lambda\right]^{-1}$$

where $P_{in}(\lambda)$ is the light power incident on the solar cell surface in a narrow range $d\lambda$ arround the wavelength λ; the first integral is the total short-circuit current density and the second integral in the denominator is the total light input.

The limit conversion efficiency $\eta_{\ell im}$, is an idealized efficiency. It describes a theoretical efficiency which is dictated only by basic phenomena and not by technique factors.

This idealized efficiency can never be reached, but is a most important tool for the evaluation of different materials or approaches.

The limit conversion efficiency $\eta_{\ell im}$ is derived based on the assumptions that there is no reflection loss, and no R_s loss. Assumed also are complete absorption of photons, 100% collection of generated electron-hole pairs. $\eta_{\ell im}$ is given as

$$\eta_{\ell im} = \frac{(V.F.)(C.F.)\frac{q}{hc}\left[\int_0^{\text{cut off}} P_{in}(\lambda)d\lambda\right]}{\int_0^{\infty} P_{in}(\lambda)d\lambda} \qquad (2.51)$$

CHAPTER 3

CHARACTERSTICS OF ELECTRICAL CONNECTIONS AND ENVIRONMENTAL INTERFACES

Experimenters usually adhere to two directions of philosophy in reporting calculated efficiencies, i.e., some report values corrected for the contact area losses and others do not. Uncorrected values are reported on philosophy that these describe what the cell can actually deliver, while efficiency values corrected for the contact area losses are reported on the basis that these are the inherent efficiencies of the devices without the human factors of contact design and process technology. Actually, it seems reasonable that both values should be reported at the same time which would eliminate ambiguity.

For enhancing the corrected-value line of thought it is essential to assess the characterstics of each of the component layers of a generalized thin film solar cell. The two semiconducting layers have been discussed in the previous chapter. In this chapter the layers which serve as electrical connections and environmental interfaces will be discussed.

3.1. Electrical contacts

3.1.1. The transparent electrical contacts

The one side of the cell which is thought to receive illumination is made up of optically transparent material which must provide an ohmic contact. At the same time it shall have a current carrying capability so as to minimize the series resistance of the total structure.

Generally, there are two basic types of transparent contacts: 1) conducting oxides such as tin oxide (TO) and mixture of indium and tin oxide (ITO), 2) open metallic grid such as silver, silver-titanium-paladium mixtures, gold, graphite, copper, nickel and chromium.

The transparent contact serves also as a substrate in the case of glass which is either covered with a conducting oxide or a metal-grid pattern. In this case the light will pass through the substrate either directly falling on the absorber-generator or going through the collector-converter to the absorber-generator.

3.1.2. Opaque electrical contacts

This electrical contact is meant to provide an electrical connection to the side of the solar cell opposite the transparent contact. It must be ohmic and low in resistivity. Hence, thin metal substrates such as copper, steel are usually preferred.

The copper layer serves also as a substrate for growing the semiconductor layers, and also as an encapsulant for one side of the device which has been developed. When serving as a substrate, it must have a coefficient of expansion that matches reasonably to its neighbouring semiconductor layers [17]. Another important characterstic is the optical reflectivity of the contact to allow multiple passes of light through the absorber-generator.

3.2. The encapsulant

Solar cells must be protected from hostile environment by an encapsulant. At the same time reflection losses introduced by this layer must be controlled. Hence, application of transparent encapsulants on one side of the solar cell meet this demand of reflection loss minimization.

In the case where the encapsulant is applied over the transparent contact, glasses have proven to be most successful. These glasses can be formed from a broad range of compounds based on silicon, oxygen, and other elements. In systems commonly used today, these glasses are bonded to a solar cell after fabrication. But development of integral encapsulants in the range of 5 μm thick directly applied to the solar cell is also taking place.

In the case of a glass substrate which also serves as a transparent contact, the encapsulant can be an opaque layer

or layers of metal, such as copper and lead, with the primary purpose of preventing environmental degradation.

3.3. Antireflection coatings

3.3.1. Analysis of reflection loss from semiconductor Layers.

The fraction of energy reflected on a boundary of a semiconducting material is determined by the reflection factor r given as

$$r = \frac{\text{reflected light intensity}}{\text{incident light intensity}} = \frac{J_r}{J_o} \qquad (3.1)$$

while the remaining

$$J(x) = J_o(1-r)e^{-\alpha x} \qquad (3.2)$$

is transmitted to a distance x in the given material where $r = r(\lambda)$ or $r(\omega)$ and $\alpha = \alpha(\lambda)$ or $\alpha(\omega)$ are the reflection and absorption spectrums of the material.

The absorption coefficient α is related to the absorption index $n\kappa$ by the expression

$$\alpha = \frac{4\pi n\kappa}{\lambda} \qquad (3.3)$$

n stands for refractive index.

From the electromagnetic theory of light the reflectivity for normal incidence can be expressed in terms of refraction and absorption indices as follows.

$$r = \frac{(n-1)^2 + n^2 \kappa^2}{(n+1)^2 + n^2 \kappa^2} \tag{3.4}$$

combining equation (3.3) and equation (3.4), we obtain

$$r = \frac{(n-1)^2 + \frac{\lambda^2}{16\pi^2}\alpha^2}{(n+1)^2 + \frac{\lambda^2}{16\pi^2}\alpha^2} \tag{3.5}$$

As is manifested in equation (3.5) the reflectivity r depends on the absorption coefficient α such that the reflectivity increases with the increase in the absorption coefficient. $r \simeq 1$, for $\kappa \gg 1$; the incident light is almsot completely reflected. This explains good light reflection by meals (metallic luster). Hence, if a substance absorbs light intensively in some spectral interval it will also intensively reflect in the same spectral interval. However, it follows from the same equation that reflection could also take place in the absence of absorption; i.e., $r \neq 0$ for $\alpha = 0$, yielding the following explicit dependence of reflectivity on refractive index.

$$r_{\alpha=0} = \frac{(n-1)^2}{(n+1)^2} \tag{3.6}$$

The majority of semiconductor materials under study for solar cells have high indices of refraction of the order of three to four as are shown in Table (3.1) below [18].

TABLE 3.1

Refractive index of some semiconductors

substance	n	substance	n
c(diamond)	2.417	InSb	3.988
Si	3.446	GaP	2.970
Ge	4.006	GaAs	3.348
InP	3.370	GaSb	3.748
InAs	3.428	AlSb	3.188

This high order or refraction index results in reflection from a planar surface in the range of 25 to 35%. In order to minimize this high reflection loss, antireflection layers are necessary.

3.3.2. Reduction of Reflection

There are two primary approaches in attempting to reduce these reflection losses.

The first technique is texturing the surface of the semiconductor so as to cause multiple reflections for incoming photons, reducing the net photon loss. The second technique is to use multilayer antireflection coatings so as to reduce reflection by both index matching and interference effects. A combination of the two techniques have also been sucessfully

utilized. It involves texturing the semiconductor layer and providing an antireflection layer on top of this material.

The deposition of several layers of appropriate indices of refraction and thickness can extend the width of the reflection minimum to near zero over a wide region, therefore leading to a highly minimized reflection loss.

The five essential layers of a solar cell described above provide all the necessary functions for the direct conversion of sunlight to electricity utilizing the photovoltaic effect.

CHAPTER 4

DESIGN OPTIONS

Any photovoltaic solar cell basically consists of the absorber generator and the collector-converter layers. On this basis, there are three design options for a single system device; namely

1) The homojunction solar cell: where the collector - converter is a semiconductor material which is of the same type as the absorber-generator,

2) The heterojunction solar cell: where the collector - converter is a semiconductor material different from the absorber-generator layer, and

3) The Schottky-barrier solar cell: where the absorber - generator is a semiconductor layer and the collector-converter is a combination of a metal and an insulator or simply metal. The energy band diagrams for these designs are shown in figure 4.1.

These three design options enable us to produce at least four distinct solar cells where each of them kick the advantage of a specific material property and/or resolve a specific material problem.

4.1. Characterstics of homojunction solar cells

In such types of solar cells, the absorber-generator and the collector-converter are made up of the same material except that the collector-converter must be of opposite conductivity to that

of the absorber-generator thus providing the barrier potential for photovoltaic energy. This barrier is a classical p/n homojunction as in the case of the common silicon single crystal cells. The number of semiconductors in which p/n homojunctions can be fabricated is limited to silicon, most $A^{III}B^{V}$ semiconductors, CdTe, ZnTe, $CuInS_2$, $CuInSe_2$ and a few others.

The homojunction has the advantage that the theory is quite well understood and some of the metallurgical and electronic problems such as thermal coefficient of expansion matching, lattice matching and electron affinity matching are overcome.

The primary problems with homojunction tends to be surface recombination at the most heavily doped surface which faces the sunlight. Good thin film cells of the homojunction type have yet to be fabricated from any other semiconductor because the diffusion process commonly used to form p/n homojunction does not work well for thin films. Diffusion down grain boundaries is difficult to control. In addition, inexpensive thin film deposition techniques like vacuum evaporation do not as a rule allow deposition of films of both conductivity types in which resistivity and other important photovoltaic parameters can be readily controlled to the degree required for efficient solar cells.

All solar cells can be described by the following equation |19|.

$$j = \Sigma j_{oi} \left(e^{\frac{qv}{n_i KT}} - 1\right) - j_L(v). \qquad (4.1)$$

Generally for a homojunction, $n_i = 1$ and j_o is given as

$$j_o = q \left(\frac{D_n}{L_n} n_{op} + \frac{D_p}{L_p} p_{on}\right) \qquad (4.2)$$

where q is the magnitude of the electronic charge, D_n the electronic diffusion coefficient, and L_n the diffusion length of electrons in the p-type material. D_p and L_p are the corresponding quantities for holes in the n-type material, n_{op} and p_{on} are the equillibrium density of electrons and holes in p-type and n-type material, respectively. j_L is the light generated current, and may be voltage dependent.

The diffusion coefficients and lengths are related to basic material properties through the equation

$$D = \frac{KT\mu}{q} \qquad (4.3)$$

$$L^2 = \frac{KT\mu\tau}{q} = D\tau \qquad (4.4)$$

where μ is the mobility and τ the recombination life time of the minority carriers.

Another mechanism which can occur is space charge region recombination with $n_i = 2$ and $j_o \sim e^{-E_g/2KT}$. The $n_i = 1$ case dominates the most efficient solar cells.

Another advantage of a homojunction is that the degradation mechanism due to interdiffusion of elements is reduced.

4.2. Characterstics of heterojunction solar cells

In a heterojunction solar cell, the collector-converter is chemically different from the semiconductor material of the absorber-generator. One of these materials is n-type and the other is p-type producing the necessary barrier voltage.

Most successful thin film cells are of the heterojunction type because they are easier to fabricate using thin film deposition techniques (Procedures) and there are many semiconductor pairs which can, in principle, produce good solar cells. Usually, the band gaps for these two materials differ significantly.

In the front-wall configuration, the small band gap material is illuminated first. Since most of the absorption will take place in this material it will control the current collected and the maximum voltage achievable. Put sometimes illumination is also carried through the larger band gap material, called the back-wall configuration.

The primary advantage of the heterojunction structure is that it allows materials which can not be doped both p-type but have other outstanding features to be utilized for very high energy conversion efficiencies, most of which are opposite conductivity type, matching electron affinities and matching of the lattice constants.

The heterojunction equation has been described by Rothworf |20| and the dominant term in equation (4.1) has the same form as the homojunction equation with $n_i = 1$ and j_o given by

$$j_o = qN_c S_I e^{-\phi/KT} \tag{4.5}$$

where S_I is the interface recombination velocity and

$$S_1 \simeq V_{th} \frac{\sigma \Delta a}{a^3} \tag{4.6}$$

where V_{th} is the thermal velocity of electrons (or holes), σ is the capture cross-section, Δa is the difference in lattice constant between the two materials, a is the average lattice constant in the plane of the junction, and ϕ is an activation energy given by the relation

$$\phi = E_{g1} - \delta_1 \; qV_{D1} - (\chi_2 - \chi_1) \tag{4.7}$$

where χ_1 and χ_2 are the electron affinities of the respective semiconductors, δ_1 the separation between the valence band and ther fermi - level in the p-type material, and V_{d1} the diffusion voltage in that material.

The main disadvantage of heterojunction structure is that, in contrast to the homojunction one, it shows a degradation mechanism due to diffusion of the component materials. Another disadvantage is revealed in the energy band diagram shown in figure (4.1b). The electron affinities of the two semiconductors

are such that a spike appears in the conduction band. This is an undesirable situation because the spike represents a barrier to the flow of minority electrons from the p-side to the n-side.

There are a variety of heterojunctions under critical investigation today. To mention a few of them, are heterojunctions such as CdS/Cu_2S, CdTe/CdS, CdS/CuInSe, InP/CdS, CuTe/CdTe, and ZnCdS/Cu_2S.

4.3. Schottky-barrier solar cells

Schottky-barrier solar cells consist of a metallic collector-converter on a semiconductor absorber-generator. This metallic contact can be on either a p-type or an n-type semiconductor. In such cells the magnitude of the diffusion potential or barrier height is determined by the difference between the work function of the metal and of the semiconductor. Now it happens that the magnitude of the diffusion potential encountered in metal - semiconductor (M-S) cells is not high enough to provide the voltages needed to extract optimum solar energy conversion performance from the semiconductor.

M-S cells can be illuminated through the metal. In such a case the metal must be very thin in order to avoid both absorption and heavy reflection losses. But if such cells are to be illuminated through the semiconductor side the metal should be of high reflectivity so as to reflect back into the semiconductor allowing thinner absorber-generator layers.

Schottky-barrier solar cell is more advantageous than either the homojunction or heterojunction since it is conceptually a simple device system, merely a semiconductor for the absorber-generator and a metal barrier. However, the mechanisms which control the behaviour of the Schottky barrier solar cell are not as well understood as the homojunction.

The main consideration is the condition of the surface of the semiconductor, the presence or abscence of an oxide or other layer between the metal and the semiconductor. Unless extreme precautions are taken, compound formation between the metal and semiconductor forms a junction, and the properties of the device are largely controlled by the properties of this layer.

The Schottky-barrier solar cells is fairly described by the equation:

$$j = A^*T^2 \, e^{-q\phi_B/KT} \left(e^{\frac{qV_j}{n_i KT}} - 1\right) \qquad (4.8)$$

with $$j_o = A^*T^2 \, e^{-q\phi_B/KT}$$

where $A^* = 120 \left(\frac{m^*}{m_o}\right) \frac{A^*}{cm^2}$ K is the Richardson constant A modified by optical phonon scattering quantum mechanical reflection, and tunneling of carriers at the metal-semiconductor interface, and m* is the effective mass tensor for the relevant

energy bands in the semiconductor. n_i is the perfection factor of the j-v characterstic of Schottky-barrier cells, and is usually greater than unity.

In general, Schottky barrier cell efficiencies are very much lower than the maximum values achieved for hetero - or homojunction cells of the same material.

4.4. Metal-insulator-semiconductor cells

One of the problems of the Schottky-barriers, the reduced open-circuit voltage, can be eliminated by using an insulator layer between the absorber-generator semiconductor and the metallic collector-converter. This insulator and metal structure serves as the collector-converter and generally yields higher open-circuit voltage than the simple Schottky configuration.

In 1974, Shewchun et al. [21] described a metal-insulator-semiconductor (M-I-S) cell consisting of a thin (≈60 Å) transparent layer of Aluminium deposited over a silicon single crystal wafer on whose surface an even thinner (≈20 Å) layer of natural silicon oxide had been grown prior to deposition of Aluminium. The oxide suppresses emission of electrons from the metal into the semiconductor but it is thin enough so that light generated minority carriers can flow from the semiconductor into the metal by tunneling.

The insulator, as mentioned above, can be an oxide or another insulating material such as a compound formed between the metal and the absorber-generator semiconductor. These devices are described as M-I-S or M-O-S depending on whether the insulator is an oxide or any other insulator.

A significant improvement over the M-I-S cell was described in 1976 by Dubow et al. [22] who replaced the transparent metal film with a conducting transparent metal film with a conducting transparent semiconductor was a mixture of indium and Tin oxide (ITO).

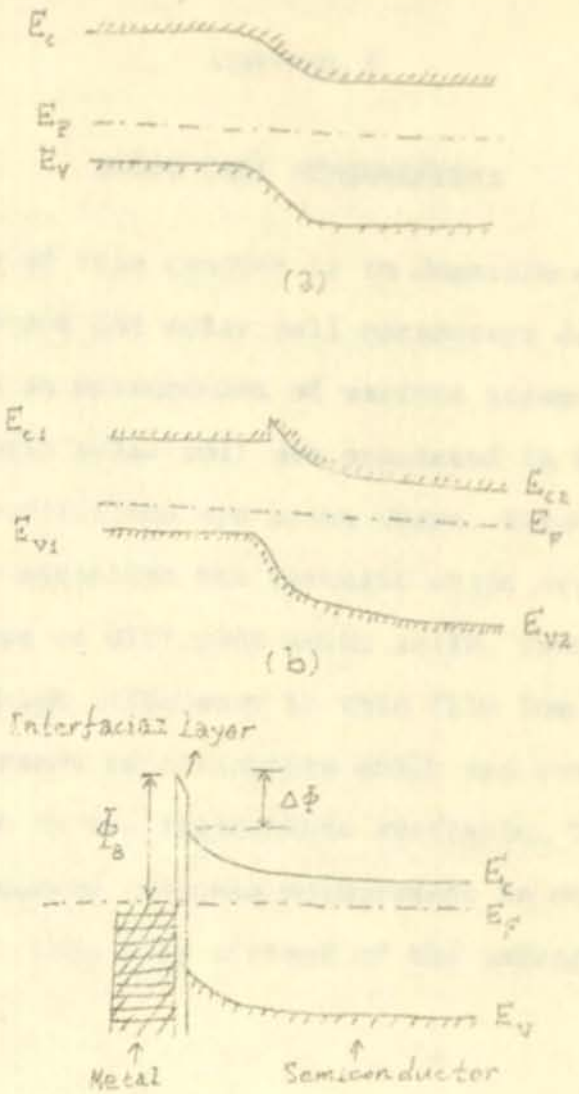

Energy band diagrams of

a) p-n homojunctions

b) p-n heterojunctions

c) MS junctions

Fig.4.1. Energy band diagrams for three possible designs of solar cells.

CHAPTER 5

SOLAR CELL MEASUREMENTS

The purpose of this chapter is to describe circuits and experimental set-ups for solar cell parameters determination. Results obtained in measurement of various parameters of FD-K Si of Soviet origin solar cell are presented in form of tables and graphs and conclusions are being drawn. Attention has been paid inorder to establish the circuits which are able to measure parameters of different solar cells, from Si-single crystal cell of high efficiency to thin film low cost cells of efficiency. The range of parameters which are covered by the circuits is given by the instruments available. Thus, for e example, the frequency response measurement is confined to the visible spectrum range only instead of the infrared and ultraviolet ones.

5.1. Efficiency measurement

Efficiency, η, of a solar cell is defined as the ratio of the maximum electrical power output, P_{max} of the cell to the incident solar power, I, on the cell.

$$\eta = \frac{P_{max}}{I} \qquad (5.1)$$

where P_{max} and I are determined by the following procedures.

5.1.1. Electrical power output determination

Efficiency, among all other parameters, is the most important quantity of a solar cell. Hence establishing ways and means of measuring this quantity experimentally is vital. To this end the circuit diagram shown in figure 5.1 was set up to measure the electrical power output of the cell.

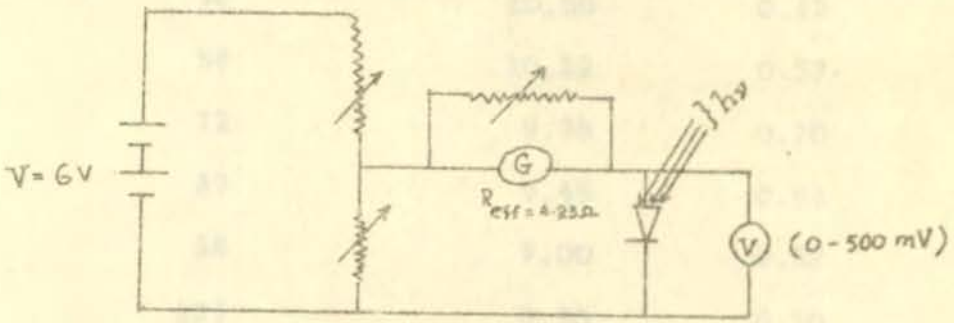

Fig.5.1. Circuit diagram for determination of electrical power output of a solar cell.

Current versus voltage readings were taken at three different levels of illumination. Illumination on the solar cell was varied by means of neutral spectral density grey filters. Results obtained from the experiment are shown in tables 5.1, 5.2, and 5.3 where the corresponding I-V curves are depicted in figure 5.2.

As calculated from the I-V data, the maximum power output of the cell for the corresponding levels of solar illumination is 1.43 mW, 0.61 mW, 0.14 mW.

Table 5.1 I-V characterstic measurement of Si-solar cell (Pd-K Si) direct sunlight illumination. Time was (10.20-10.30 a.m.)

V [mV]	I [mA]	P [mW]
0	10.50	0.00
40	10.50	0.42
56	10.12	0.57
72	9.78	0.70
87	9.45	0.82
58	9.00	0.52
121	8.70	0.10
133	8.43	0.11
150	8.10	0.12
164	7.76	1.27
179	7.45	1.33
200	7.00	1.40
221	6.40	1.41
237	6.05	1.42
251	5.70	1.43
260	5.49	1.42
276	5.10	1.41
291	4.72	1.37
303	4.40	1.33
313	3.11	1.29

Table 5.1 (continued)

V [mV]	I [mA]	P [mW]
330	3.65	1.20
351	3.02	1.06
338	2.48	0.84
385	2.00	0.76
393	1.70	0.67
402	1.40	0.56
408	1.20	0.49
411	1.00	0.41
416	0.80	0.33
435	0.00	0.00

Table 5.2 I-V characterstic measurement of Si-solar cell (Pd-K Si) under sunlight illumination (Intensity reduced by one-fourth). Time was 10.30-10.35 a.m.

V [mV]	I [mA]	P [mW]
10	3.06	0.31
30	3.04	0.91
72	3.02	0.22
112	3.01	0.34
135	3.00	0.41
153	2.99	0.46
172	2.94	0.51
190	2.86	0.54
244	2.40	0.59
280	2.17	0.61
301	1.85	0.56
307	1.67	0.51
320	1.52	0.49
354	1.28	0.45
341	1.10	0.38
335	0.90	0.30
380	0.00	0.00

Table 5.3 I-V characterstic measurement of Si-solar cell (Fd-K Si) under sunlight illumination (Intensity reduced by one-sixteenth). (Time was 10.40-10.45 a.m.).

V [mV]	I [mA]	P [mW]
0	0.75	0.00
30	0.74	0.02
72	0.73	0.05
113	0.73	0.08
144	0.72	0.10
175	0.72	0.13
191	0.71	0.14
196	0.71	0.14
343	0.00	0.00

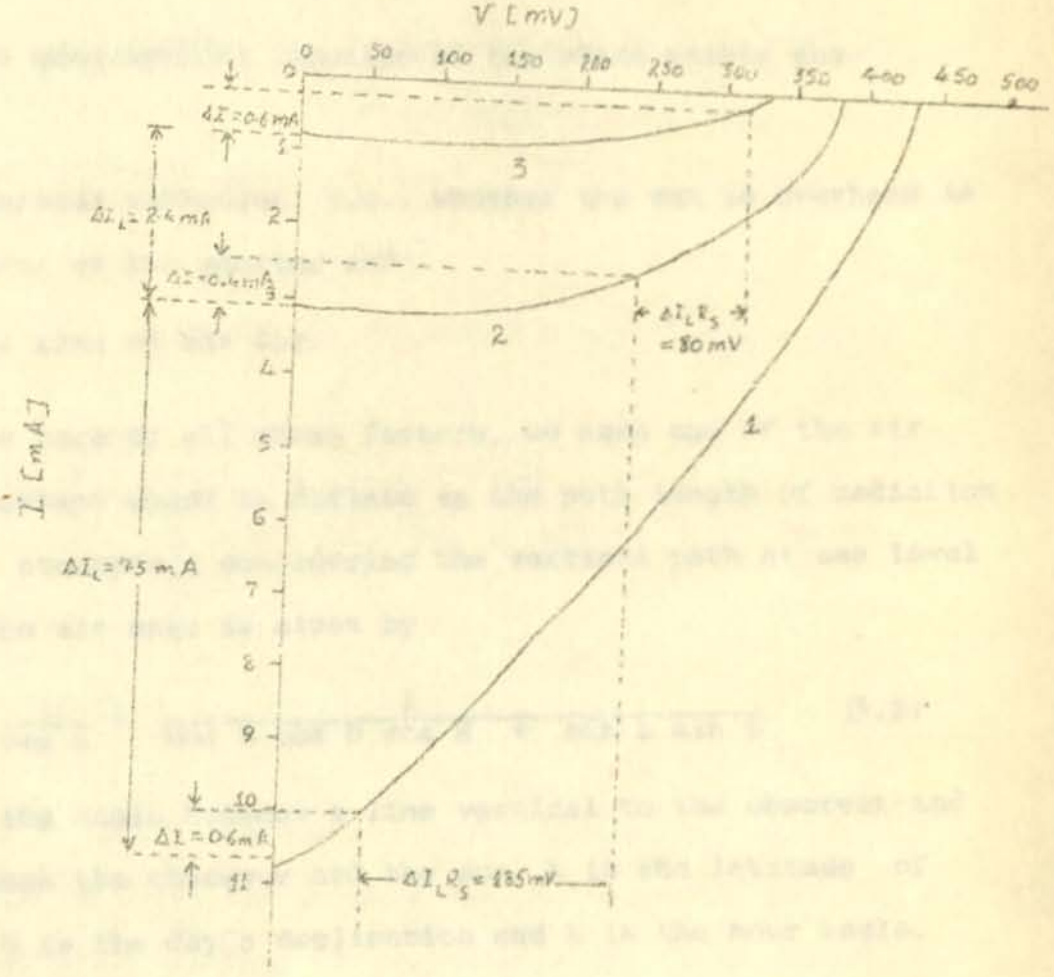

Fig.5.2. Photovoltaic output characterstics.

5.1.2. Incident solar power determination

The estimate of the incident solar irradiance at the earth's surface is 95.6 mW/cm^2 for the sun directly overhead. The suns's irradiance vary due to the following main factors,

1) The geographical location of the place mainly the latitude,

2) Seasonal variation, i.e., whether the sun is overhead in the tropics or at the equator and

3) The time of the day.

To take care of all these factors, we make use of the air mass (AM) concept which is defined as the path length of radiation through the atmosphere considering the vertical path at sea level as unity. The air mass is given by

$$AM = \frac{1}{\cos z} = \frac{1}{\cos L \cos D \cos H + \sin L \sin D} \qquad (5.2)$$

where z is the angle between a line vertical to the observer and a line through the observer and the sun. L is the latitude of the place, D is the day's declination and H is the hour angle.

1) The local latitude (L) for Addis Ababa is 9^{o}

2) The day's declination of the sun (D) is given by

$$D = 23.5^{o} \sin\left(\frac{n\pi}{365}\right) \qquad (5.3)$$

where n is the number of days from vernal equinox measured plus or minus according to whether the sun is north or south of the equator, respectively. On June 7, n = 79 days.

Thus, $D = 23.5^{\circ} \sin \frac{79\pi}{365} = 14.8^{\circ}$.

3) The hour angle H is determined by taking the arctangent of the ratio of the height, h, of a given object to the average length of its shadow, I.

$$H = \tan^{-1}\left(\frac{h}{\bar{I}}\right) \qquad (5.4)$$

where $h = 12.0$ cm, $\bar{I} = 9.75$ cm and $H = \tan^{-1}\left(\frac{12}{9.75}\right) = 50.9^{\circ}$.

Therefore,

$$\cos z = \cos L \cos D \cos H + \sin L \sin D$$
$$= \cos 9 \cos 14.8 \cos 50.9 + \sin 9 \sin 14.8$$
$$= 0.6422.$$

$$AM = \frac{1}{\cos z} = 1.6.$$

The solar irradiance for the above calculated air mass can be obtained from the graph shown in figure 5.3 which is found in any standard book of astronomy, and is 86 mW/cm^2.

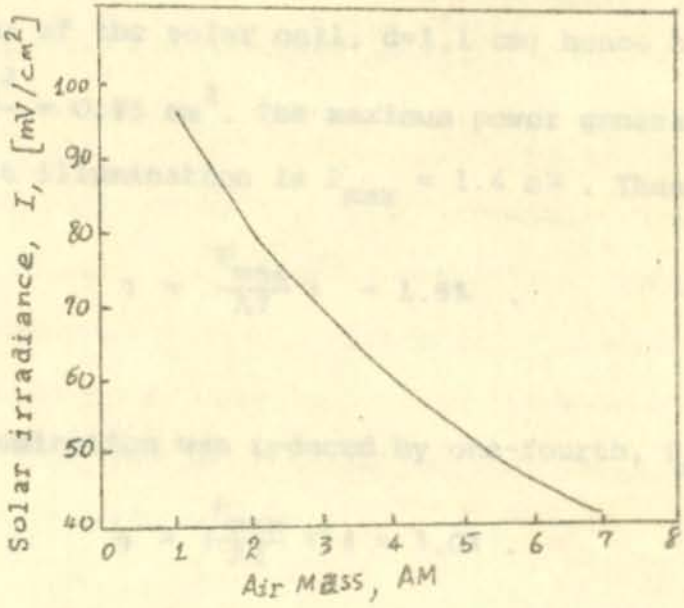

Fig.5.3. Solar irradiance versus Air Mass

5.1.3. Calculation of efficiency

Once the electrical power output of the cell and the solar irradiance on the cell were determined its conversion efficiency could be obtained as follows.

$$\eta = \frac{\text{max. Power output/unit area}}{\text{Solar-irradiance}} \times 100 = \frac{P_{max}}{AI} \times 100.$$

Diameter of the solar cell, d=1.1 cm; hence had a total area $A = \frac{\pi d^2}{4} = 0.95\ cm^2$. The maximum power generated under visible light illumination is $P_{max} = 1.4$ mW . Thus,

$$\eta = \frac{P_{max}}{AI}\ \% = 1.8\% \ .$$

When the illumination was reduced by one-fourth, $P_{max} = 0.61$ mW

and $$\eta = (\frac{P_{max}}{AI}\ \%)4 = 3.0\% \ .$$

When the illumination was again reduced by one-sixteenth

$P_{max} = 0.14$ mW

and $$\eta = (\frac{P_{max}}{AI}\ \%)16 = 2.7\% \ .$$

Such a low efficiency is attributed to the internal series resistance of the cell. From the I-V characterstic shown in figure 5.2 an easy and accurate determination of this internal resistance could be made according to the method employed by Martin Wolf and Hans Rauschenbach |23|.

The two photovoltaic output characterstics are translated against each other by the amounts ΔI_L (Light generated current) and $\Delta I_L R_S$ (potential drop across the internal resistance) in the y- and x- directions, respectively. Two corresponding points on the two characterstics show a displacement with respect to each other, which is identical to the two translations of the coordinate systems. The displacement parallel to the ordinate gives the value of ΔI_L. Since the displacement parallel to the abscissa equals $\Delta I_L R_S$, the value of the internal resistance R_S is readily obtained.

One practical approach to this procedure is to choose an arbitrary interval ΔI from the short-circuit current which determines the first characterstic. It is frequently found convinient to choose ΔI so as to obtain a point in or near the knee of the characterstic. The same ΔI value is used for finding a second corresponding point on the second characterstic curve.

Applying this method of correlation a shift of $\Delta I = 0.6$ mA is made from the short current $I_{sc} = 10.5$ mA and $I_{sc} = 3.1$ mA of curves (1) and (2) corresponding voltage shifts $\Delta I_L R_S = 185$ mV and $\Delta I_L R_S = 80$ mV are obtained from the curves. The change in the light generated current between characterstic curves (1) and (2) is 7.5 mA. Hence the internal resistance of the cell which ofcourse includes that of the ammeter is obtained to be $R_S = \Delta I_L R_S / \Delta I_L = 24.6\Omega$. If correction of the internal resistance of the ammeter ($R=4.13\Omega$) is made the internal resistance of the cell alone becomes $R_S = 20.4\Omega$.

Similarly performing the same translation on curves (2) and (3), and effecting the correction due to the ammeter the internal resistance of the cell happens to be 29.2Ω.

The curves in figure 5.2 indicate that the internal resistance can severely affect the performance of photovoltaic cells as solar energy converters. The maximum power output of a solar cell is given by the area of the largest rectangle that can be drawn inside the photovoltaic output characterstic. The area of such a rectangle increases with increasing sharpness of the knee in the photovoltaic output characterstic. Internal series resistance causes a successively larger rounding of the curve at increasing light intensities.

The knee of each of the characterstic curves represent the maximum power point voltage. As reavealed in the curves obtained, this point decreases with increasing light intensity due to the finite internal series resistance of the cell.

The effect of the internal series resistance on the short circuit current of the cell is also evident. In actuality, the short circuit current must be directly proportional to the increase in light intensity. But as shown in the photovoltaic characterstic curves, for a constant increase of illumination, the increase in short circuit current decreases. Hence, it is not correct to assume that the short-circuit current is always equal to the light generated current at every level of illumination.

5.2. Spectral response measurement

Another important parameter of a solar cell is its response to various wavelength radiations. Since the solar spectrum consists of various wavelength radiations it is instructive to study the behavior of spectral response of a solar cell.

Spectral response is defined as the short-circuit current per incident light power versus wavelength or photon energy. Some authors like Cusano [24] define the spectral response as the short-circuit current per number of incident photons.

As the light source it was used an incandescent tungsten filament lamp operating at 5.6v. The temeprature of the filament was determined earlier by Letemeskel to be 2400K[25].

The spectral emittance, $M(\lambda,T)$ for tungsten is given by formula

$$M(\lambda,T)_t = e(\lambda,T) \quad M(\lambda,T)_{bb} \tag{5.5}$$

where $e(\lambda,T)$ is tungsten spectral emissivity and $M(\lambda,T)_{bb}$ is the spectral emittance of a black body radiator. The spectral dependence of $e(\lambda,T)$ for $T = 2400K$ is indicated in figure 5.4 according to Wyszechi and Shiles [26].

Grating monochromator (Coleman 6A Junior Spectrophotometer) was used for spectral response measurement. Short-circuit

photocurrent was measured at different wavelengths within the range of 400 nm to 700 nm. Photocurrent as low as 10^{-10}A could be measured with Griffin d-c amplifier and electrometer available. Results obtained are tabulated in table 5.4 and shown in figure 5.5.

The spectral energy distribution derived from figure 5.4 was used to normalize the cell photocurrent (Table 5.4) and given in table 5.5. Results of relative spectral response measurements show that Si solar cells are highly responsive within the visible spectrum as shown in figure 5.5b.

Table 5.4 Spectral response of Fd-K Si solar cell

λ [nm]	I_a [arbitrary unit]	E [ev]
400	0.60	3.10
410	0.80	3.02
420	1.00	2.96
430	1.40	2.89
440	1.60	2.82
450	2.00	2.76
460	2.60	2.70
470	2.80	2.64
480	4.00	2.59
490	5.00	2.53
500	6.00	2.48
510	6.80	2.43
520	8.40	2.39
530	10.0	2.34
540	12.0	2.30
550	14.0	2.26
560	17.6	2.22
570	20.0	2.18
580	24.0	2.14
590	27.0	2.10
600	30.4	2.07
610	34.0	2.03
620	38.0	2.00
630	43.0	1.97

Table 5.4. (continued)

λ [nm]	I_a [arbitrary unit]	E [ev]
640	47.0	1.94
650	51.0	1.91
660	56.0	1.88
670	60.0	1.85
680	64.0	1.83
690	69.0	1.80
700	73.5	1.77

Table 5.5 Normalized spectral response of Fd-K Si solar cell

λ [nm]	$y=\log(\frac{M_{2400}}{M_{300}})$	10^y	I_a [arbitrary unit]	$I_a/10^y$
400	0.45	2.82	0.60	0.21
420	0.65	4.47	1.00	0.22
440	0.83	6.69	1.60	0.24
460	1.00	10.00	2.60	0.26
480	1.13	13.34	4.00	0.30
500	1.27	18.84	6.00	0.32
520	1.38	23.71	8.40	0.35
540	1.48	29.85	12.00	0.40
560	1.58	37.58	17.60	0.47
580	1.65	44.67	24.00	0.54
600	1.73	53.09	30.40	0.57
620	1.80	63.10	38.00	0.60
640	1.88	74.99	47.00	0.63
660	1.93	84.14	56.00	0.67
680	1.98	94.41	64.00	0.68
700	2.03	105.93	73.50	0.69

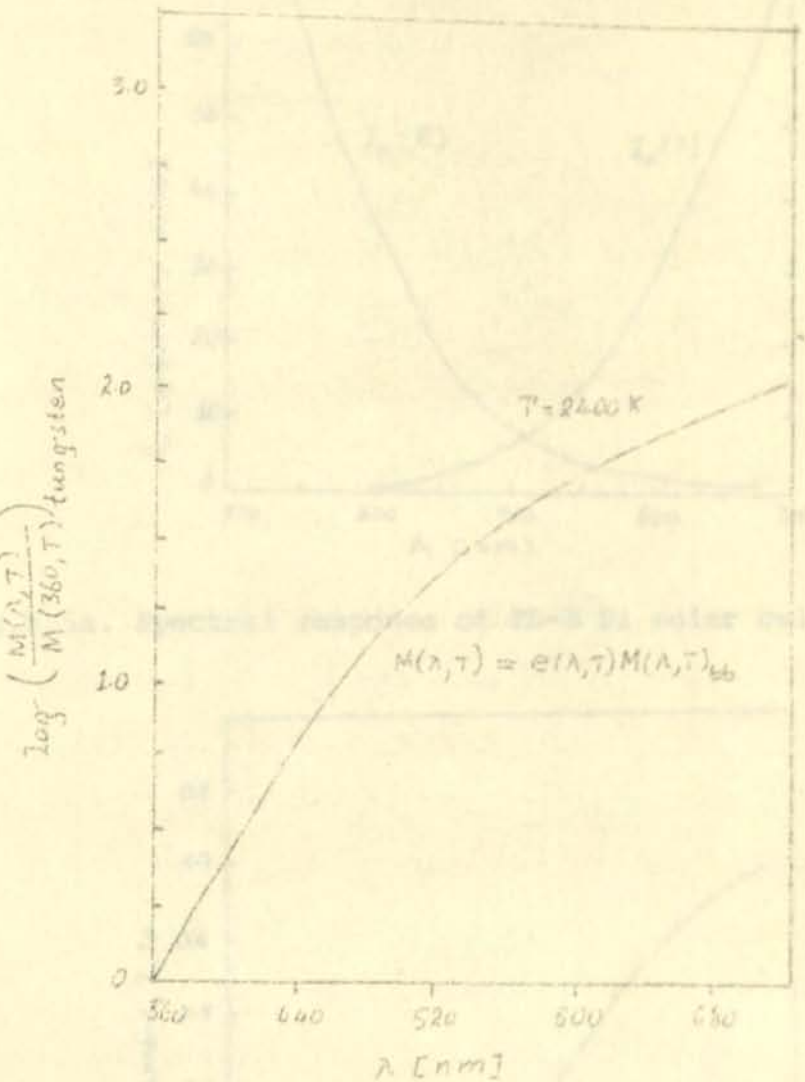

Fig.5.4. Relative spectral energy distribution of incandascent tungsten lamp.

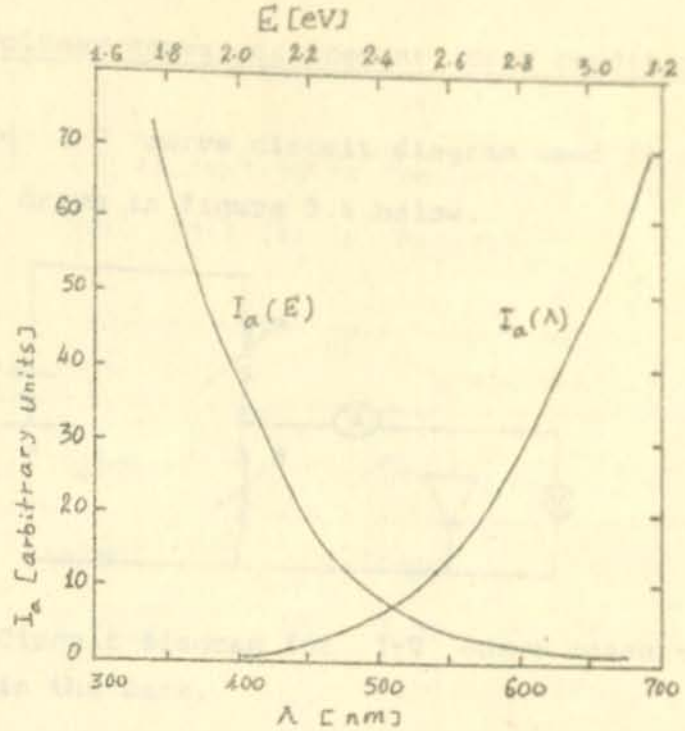

Fig.5.5a. Spectral response of FD-K Si solar cell.

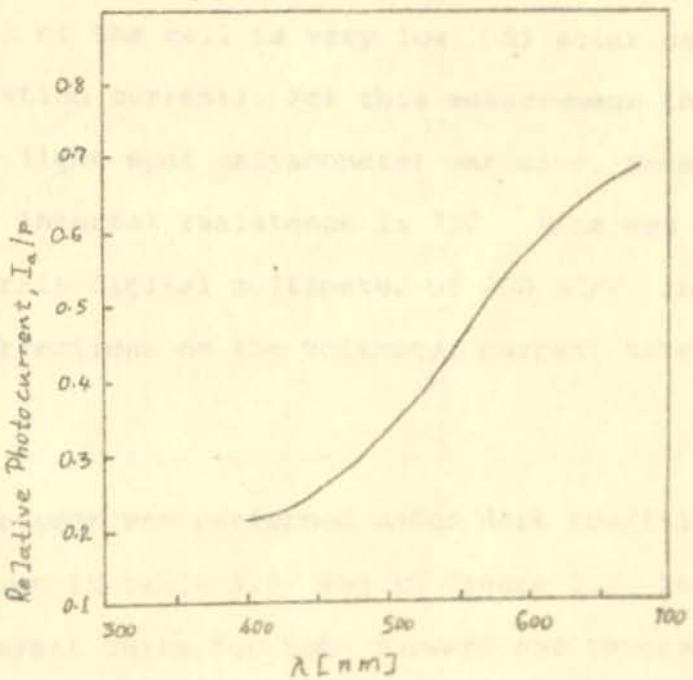

Fig.5.5b. Normalized spectral response FD-K Si solar cell.

5.3. Current-voltage curve measurement (dark conditions)

A standard I-V curve circuit diagram used in our measurement is drawn in figure 5.6 below.

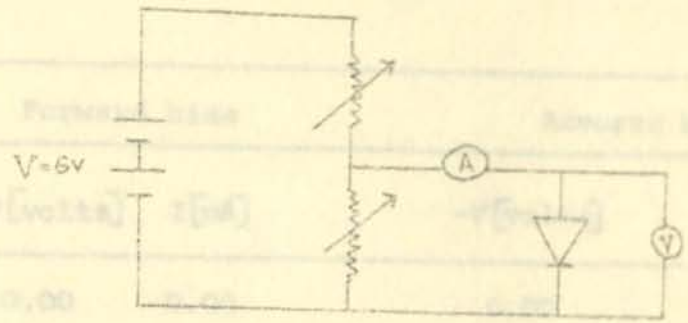

Fig.5.6. Circuit diagram for I-V curve measurement in the dark.

Resistor decades boxes were used to control the solar cell bias. Forward current was measured by a d.c. milliammeter. Reverse current of the cell is very low (Si solar cell has very low saturation current). For this measurement the WPA Soffron Walden light spot galvanometer was used. Sensitivity is 72.5 mm/μA, internal resistance is 75Ω. Bias was measured by Phillip Harris digital multimeter of 200 KΩ/V internal resistance. Corrections on the voltmeter current have been made.

The measurement was performed under dark conditions. The results are given in table 5.6 and in figure 5.7. The current axes have different units for both forward and reverse bias.

Table 5.6 I-V characterstic measurement of Si-solar cell (Fd-K Si) in the dark

Forward bias		Reverse bias	
V[volts]	I[mA]	-V[volts]	I[nA]
0.00	0.00	0.00	0.00
0.35	0.20	0.10	70.00
0.40	0.90	0.20	100
0.46	1.20	0.30	110
0.50	2.30	0.40	120
0.64	9.00	0.50	140
0.70	12.0	0.60	150
0.80	26.0	0.70	160
0.90	50.5	0.80	165
1.00	82.5	0.90	170
		1.00	172
		1.20	180

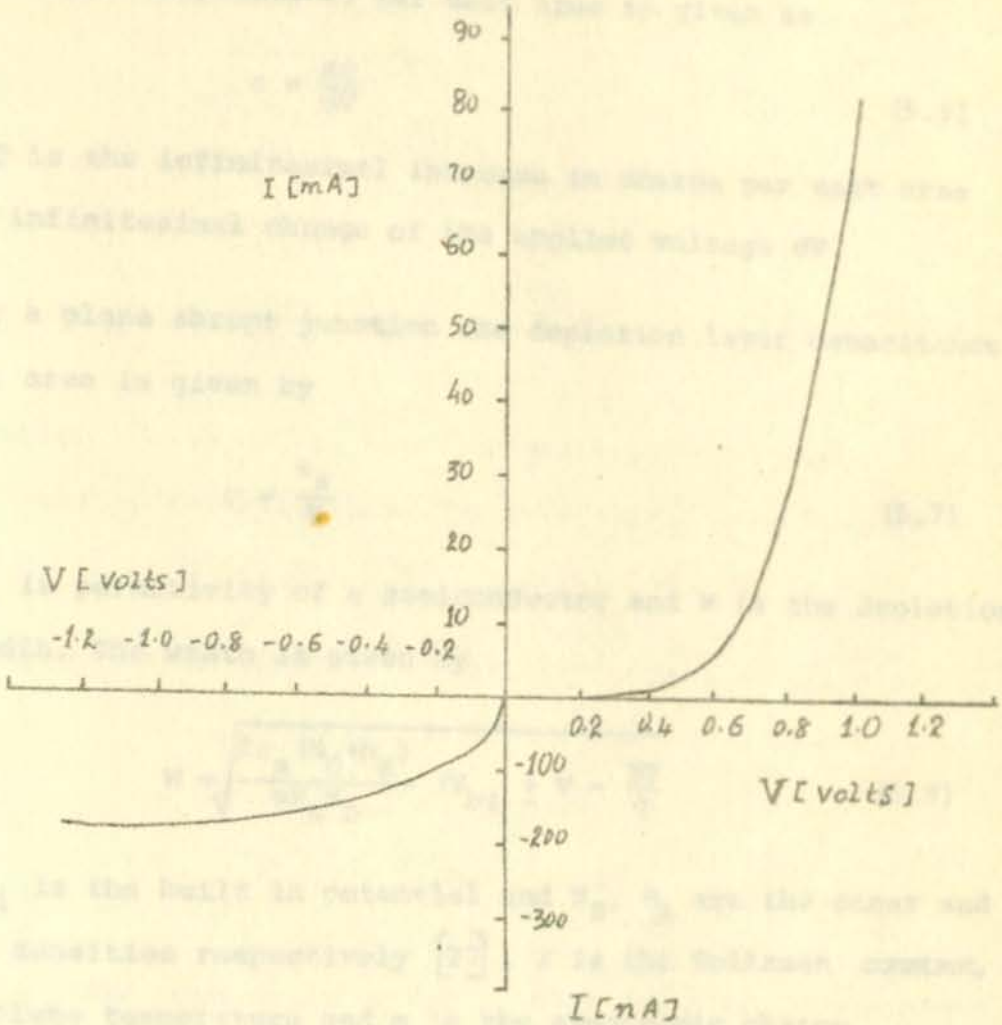

Fig.5.7. I-V characterstic curve of FD-K Si solar cell, in the dark.

5.4. Capacitance-voltage curve measurement

The depletion layer of a junction device represents a capacitor whose capacitance per unit area is given as

$$c = \frac{dQ}{dV} \tag{5.6}$$

where dQ is the infinitesimal increase in charge per unit area upon an infinitesimal change of the applied voltage dV.

For a plane abrupt junction the depletion layer capacitance per unit area is given by

$$c = \frac{\varepsilon_s}{W} \tag{5.7}$$

where ε_s is permitivity of a semiconductor and W is the depletion layer width. The width is given by

$$W = \sqrt{\frac{2\varepsilon_s (N_D+N_A)}{qN_AN_D}\left(V_{bi} \pm V - \frac{KT}{q}\right)} \tag{5.8}$$

where V_{bi} is the built in potential and N_B, N_A are the donar and acceptor densities respectively [27]. K is the Boltzman constant, T is absolute temperature and q is the electronic charge.

In the case of a one-sided abrupt junction, the above expression reduces to

$$W = \sqrt{\frac{2\varepsilon_s V_{bi}}{qN_B}} \tag{5.9}$$

where N_B is equal to the donor density N_D or the acceptor density N_A depending on whether $N_A >> N_D$ or vice versa.

Combining equations (5.7), (5.8) and (5.9) one obtains

$$C = \sqrt{\frac{q\varepsilon_s N_B}{2\left(V_{bi} \pm V - \frac{KT}{q}\right)}} \tag{5.10}$$

or

$$\frac{1}{C^2} = \frac{2}{q\varepsilon_s N_B}\left(V_{bi} \pm V - \frac{KT}{q}\right) \tag{5.11}$$

Equation (5.11) can be used for the built-in potential (barrier height) determination. The term KT/q is negligible (for 300 K, it is equal to 26 mV).

Differentiating equation (5.11) with respect to V, one obtains

$$\frac{d\left(\frac{1}{C^2}\right)}{dV} = \pm \frac{2}{q\varepsilon_s N_B} \tag{5.12}$$

It is clear from equation (5.11) that a C-V curve measurement furnishes a lot of important data of the junction. Hence, measurement was performed with an impedance bridge (1650-A General Radio Corporation). The measurement frequency was 1.00 KHZ. Reverse cell bias was within the range of 0 to 6 volts. The circuit diagram is shown in figure 5.8.

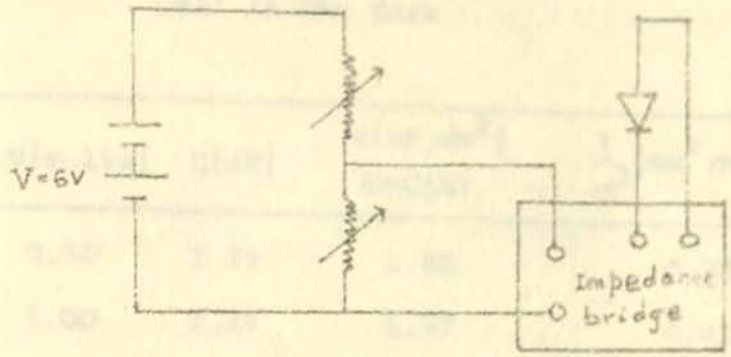

Fig.5.8. Circuit diagram for C-V curve measurement.

The measurement was performed under dark and illuminated conditions. C-V and $\frac{1}{C^2}$ -V curves are shown in figures 5.9 and 5.10 as produced from tables 5.7 and 5.8.

The built-in potential V_{bi} is determined by extrapolating the straight line curve (1) to the positive voltages axis and is found to be 0.75 eV . From the slope of the straight line curve the donor density N_D in the cell is obtained to be $3.53 \times 10^{+19} m^{-3}$.

Table 5.7 C-V characterstic measurement of Pd-P Si solar cell in the dark

-V|volts|	C|nF|	c|nF/cm^2| (c=C|A)	$\frac{1}{c^2}$|cm^2/nF|^2
0.50	1.79	1.88	0.28
1.00	1.49	1.57	0.41
1.50	1.32	1.39	0.52
2.00	1.19	1.25	0.64
2.50	1.10	1.16	0.75
3.00	1.02	1.07	0.87
3.50	0.96	1.01	0.98
4.00	0.94	0.99	1.02
4.50	-	-	-
5.00	0.86	0.89	1.22
5.50	-	-	-
6.00	0.78	0.82	1.48

Table 5.8 C-V characterstic measurement of Pd-K Si solar cell under illumination by Tungsten filament

-V[volts]	C[nF]	C|nF/cm^2 (c = C|A)	$\frac{1}{c^2}$|cm^2/nF|^2
2.50	1.84	1.94	0.27
3.00	1.54	1.62	0.38
3.50	1.26	1.43	0.49
4.00	1.24	1.30	0.59
4.50	-	-	-
5.00	1.05	1.10	0.82
5.50	-	-	-
6.00	0.94	0.99	1.02

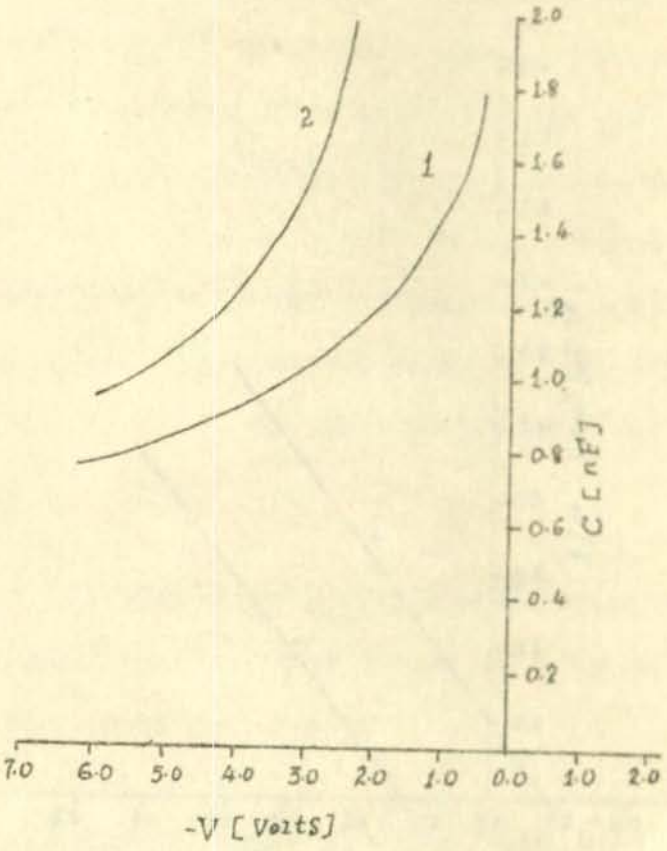

Fig.5.9. C-V characterstic curves.

1) In the dark

b) Illuminated.

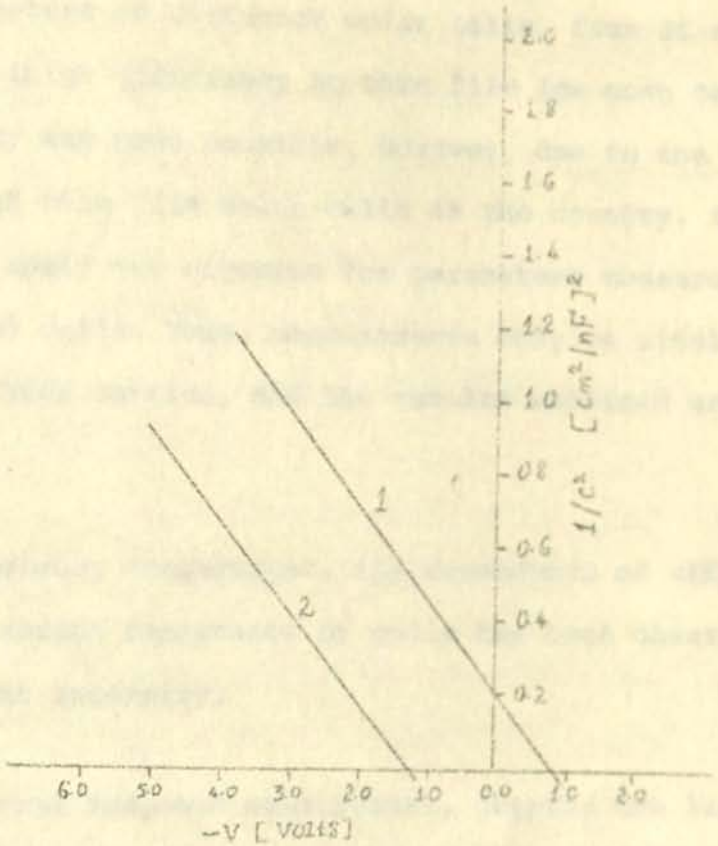

Fig.5.10. $\frac{1}{C^2}$ versus V curve.

CONCLUSION

In this work the establishment of circuits which are able to measure parameters of different solar cells, from Si-single crystal cell of ihigh efficiency to thin film low cost cells of low efficiency was made possible. However, due to the inavailability of thin film solar cells in the country, it was not possible to apply our circuits for parameters measurement of these types of cells. Thus, measurements only on single Si solar cell have been carried, and the results obtained are acceptable.

In the efficiency measurement, the dependence of efficiency on the internal series resistance of cells has been observed to vary with light intensity.

In the spectral response measurement, despite the limited range of the spectrophotometer used, a good information about the sample cell could be drawn; i.e., the cell shows a rapid increase in spectral response upto the middle of the visible range, then the increase is gradual.

REFERENCES

1. Becquerel, E., "On Electrics effects under the influence of solar radiation", Compt. Rendl, Vol.9 p.561, 1839.

2. Adams, W.G., and Day, R.E., "The action of light on selenium, "Proc. Roy. Soc., Vol. A 25, p.113, 1877.

3. Lange, B., "New photoelectric cell", Zeit. Phys. Vol.31, p.139, February, 1930.

4. Grondahl, L.O., "The copper-cuprous-oxide rectifier and photoelectric cell", Rev. Mod. Phys., Vol.25, p.141, April, 1933.

5. Schottky, W., "Cuprous oxide photoelectric cells", Zeit. Phys., Vol.31, p.913, November, 1930.

6. Rapport, P., "The electron-voltaic effect in p-n junctions induced by Beta particle bombardment", Phys. Rev., Vol.93, p.246, January, 1954.

Rapport, P., Lofferski, J.J., and Linder E.G. "The electron-voltaic effect in germanium and silcon p-n junctions", RCA Review, Vol. XVII, p.100, March, 1956.

7. Chappin, D.M., Fuller, C.S., and Pearson, G.L., "A new silicon p-n junction photocell for converting solar radiation into electrical power", J. Appl. Phys., Vol.25, p.676, May, 1954.

8. Reynolds, D.C.; Leies G., Antes, L.L., and Murburger R.E., "Photovoltaic effect in cadmium sulphides", Phys. Rev., Vol.96, p.533, October, 1954.

9. Lofferski, J.J., "Thin films and solar energy applications", Surface Science 86 (1979) 424-443.

10. Baso, B.M. "High-efficiency electroplated heterojunction solar cell", J. Appl. Phys.,55(2), 15 January, 1984.

11. Isett, L.C., "Annealing of CdS/CdTe solar cells", J. Appl. Phys., 55(8), 15 April, 1984.

12. Ki Hyun Yoon and Sang OK Yoon, "Photoeffects in polycrystalline TiO_2 electrodes", Japanese Journal of applied physics, Vol. 23, No.8, August, 1984, p.1137-1140.

13. Novel, N.J., Semiconductors and semimetals. New York, Harcourt Brace Jovanovich, Publishers, 1975.

14. Schockley, W., Electrons and holes in semiconductors. p.318. Van Nostrand, Princeton, New Jersey, 1950.

15. Barnet, A.M., "Thin film solar cells: A unified analysis of their potential", IEEE transactions on Electron device. vol. 27, No.4, 615-30, April, 1980.

16. Wolf, M., "Limitations and possibilities for improvement of photovoltaic solar energy converters", Proc. IRE, Vol. 48, 1246-63, July, 1960.

17. Schockley, W., Electrons and holes in semiconductors D.Van Nostrand Co. Inc., New York, p.309-15, 1954.

18. Kireev, P.S., Semiconductor Physics. Moscow: Mir publishers, 1975.

19. Alfman, M., Elements of solid-state energy conversion. Van Nostrand. Reinhold Company, 1969.

20. Rathworf, A., "Research directed to stable high efficiency CdS solar cells", Tech. Rep. NSF/RANN/AER 72-03478 AO3/TR/75/3, May, 1975.

21. Schewchun, J., et al, Solid state electrone. Vol. 7 p.563, 1974.

22. DuBow, J.B., et al., Appl. Phys. Letters Vol. 29, p.494, 1976.

23. Wolf, M., and Rauschenbach, H., "Series resistance effects on solar cell measurements", Advanced energy conversion. Vol. 3, p.455-79. June, 1963.

24. Cusano, D.A., "CdTe solar cells and photovoltaic heterojunctions in II-VI compounds", solid state electron, Vol.6, p.217-232, June, 1963.

25. Letemeskel Asfaw "Investigation of photoconductivity in CdS", M.Sc. thesis, 1984, (unpublished) , AAU.

26. Wyszecki, G., Stiles, W.S., Color science, New York: John Wiley and Sons Inc., 1967.

27. Sze, S., Physics of semiconductor devices. New York: Jonh Wiley and Sons, 1969.

DECLARATION

I hereby declare that the thesis entitled, "Theoretical and Experimental Study of the Photovoltaic Effect in thin films", being submitted by me in partial fulfillment for Master of Science Degree in Physics, is my original work, done under the supervision and guidance of Dr. P. Hruska. Sources of relevant findings and equations taken from books and articles are duly acknowledged in the body of the thesis and the reference.

Gebre Hiwet Embaye

The thesis was submitted to
the Physics Department Graduate
Committee in June, 1985

This thesis has been submitted for examination with my approval as University Advisor.

P. Hruska, Ph.D.